

The expression level of rat M-cadherin was compared between TR-iBRB and TR-BBB cells. Following quantitative real time PCR analysis using rat M-cadherin specific primers amplified at nucleotide position 790-916, the rat M-cadherin mRNA content relative to the amount of GAPDH mRNA (M-cadherin/GAPDH) in TR-iBRB2, TR-iBRB9, TR-BBB11, and TR-BBB13 cells was $2.38 \pm 0.41 \times 10^{-3}$, $6.93 \pm 0.67 \times 10^{-3}$, $7.32 \pm 4.80 \times 10^{-5}$, and $2.74 \pm 0.49 \times 10^{-5}$, respectively (Figure 3A). The mean value of the rat M-cadherin mRNA content in TR-iBRB cells was 92.9 fold greater than that in TR-BBB cells. Consistent with mRNA expression, immunoblot analysis revealed that the expression of rat M-cadherin protein at 130 kDa in TR-iBRB cells was greater than that in TR-BBB cells (Figure 3B). The molecular weight of rat M-cadherin at 130 kDa was identical to the reported value for rat L6 myoblasts [14].

DISCUSSION

This study found eight genes expressed more in retina than in brain capillary endothelial cell lines using mRNA differential

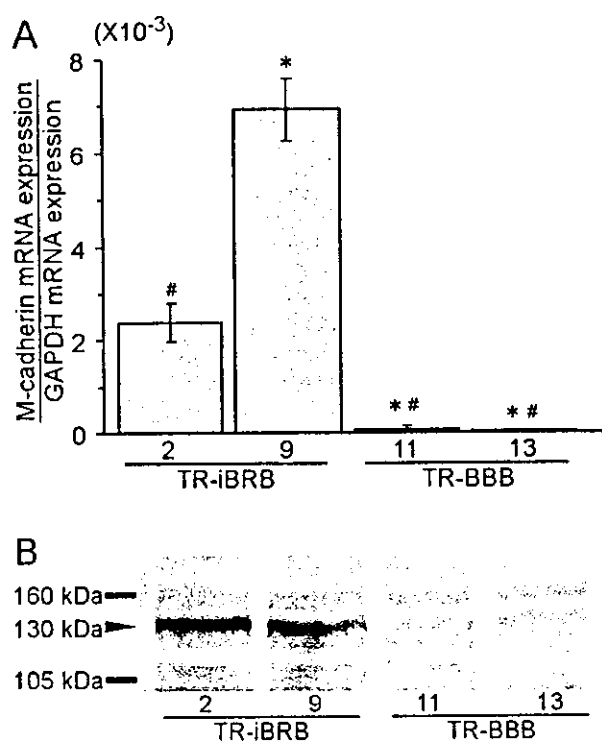


Figure 3. Expression of rat M-cadherin in TR-iBRB and TR-BBB cells. **A:** Quantitative real time PCR analysis of rat M-cadherin. The rat M-cadherin mRNA expression level was normalized by the GAPDH mRNA expression. Each point represents the mean of 3-4 observations. The error bars represent the standard error of the mean. An asterisk (***) indicates $p < 0.01$ for the comparison to TR-iBRB2 cells. A sharp sign (“#”) indicates $p < 0.01$ for the comparison to TR-iBRB9 cells. **B:** Immunoblot analysis of rat M-cadherin. One representative immunoblot analysis from three independent experiments is shown.

display analysis with 48 primer combinations (Table 1). Three hundred primer combinations are required to visualize all differentially displayed genes [15]. Therefore, 16% of mRNAs in both cell lines were screened in this study, and further 42 genes are expected to exist as a differentially displayed gene in TR-iBRB cells. For the analysis of differentially displayed genes between the inner BRB and BBB, it is important to use cells exhibiting normal physiological properties. In the case of isolated capillary endothelial cells from animals, it is difficult to avoid contamination from non-endothelial cells and obtain a sufficient number of cells due to very small dimensions of the retina. Using TR-iBRB and TR-BBB cells eliminates these concerns, since both cell lines were established from the same rat strain using the same procedure and cultured in the same conditions. Moreover, both cell lines possess the same endothelial markers and express several transporters [9-11], which have been reported to be expressed in vivo retinal and brain capillaries [2,3,6,7]. Therefore, the difference in expressed genes between these cell lines may indeed reflect the difference between the inner BRB and BBB in vivo.

Cadherin is an adherens junction protein and mediates calcium dependent cell-cell adhesion in a homophilic manner [16]. It has been reported that some cadherin-family proteins are expressed at the inner BRB and the BBB. VE-Cadherin (cadherin-5), an endothelial cell specific protein which is necessary for vessel formation in vivo [17], is localized to adhesion sites of endothelial cells in the retina and brain [18,19]. In embryonic chicken brain and retina, N-cadherin (cadherin-2) is expressed at contact zones between pericytes and endothelial cells and its concentration rapidly falls with the onset of barrier differentiation, suggesting that N-cadherin expression represents a signal for the expression of barrier properties [20]

The present study revealed that M-cadherin is highly expressed in TR-iBRB cells, but not in TR-BBB cells (Figure 3). TR-BBB cells originate from the cerebrum, and there is no report of M-cadherin being expressed in the cerebrum. On the other hand, when *nls-lacZ* reporter gene was introduced into the M-cadherin locus, strong β -gal activity was observed in the distinct cell layer of the retina [21], suggesting that M-cadherin is expressed in the retina. Ultrastructural comparison between the retinal and brain capillaries shows that retinal vessels have denser interendothelial junctions and a greater covering of pericytes than brain vessels [1]. In diabetes, the neovascularization following the loss of pericytes from vessels mostly occurs in the inner BRB, and may not take place in the BBB [22]. It is proposed that M-cadherin is intimately involved in these ultrastructural and pathological differences in cell-cell adhesion between the inner BRB and BBB.

Rat M-cadherin, which has been cloned for the first time, contains a hydrophobic signal sequence at amino acids 1-21 [23] and a postulated furin cleavage site of precursor polypeptides at amino acids 44-45 [23]. The deduced 740 amino acid sequence of mature M-cadherin protein consists of a long extracellular domain containing five cadherin extracellular subdomain repeats (EC1-EC5), a transmembrane domain, and a cytoplasmic domain. The extracellular domain of M-cadherin

includes the characteristic cadherin consensus sequences DXD, LD(R/Y)E, and DXNDNXP which are involved in Ca²⁺ binding [24]. Furthermore, four cysteine residues conserved in cadherin are also present in the EC5 of M-cadherin. There are five N-glycosylation sites in the extracellular domain. The cytoplasmic domain of M-cadherin includes a membrane-proximal conserved domain (MPCD) [16], which is implicated in the basolateral sorting of cadherin molecules, and a catenin binding sequence (CBS) [16].

The 3' termini of GATA-3 and BCATc mRNAs were expressed 24 and 5.5 fold more in TR-iBRB than TR-BBB cells, respectively. A transcription factor, GATA-3, is predominantly expressed and required for optimal cytokine production in T helper type 2 cells [25]. Although the physiological role of GATA-3 at the inner BRB is not clear at the present time, GATA-3 may regulate the expression of some genes that are responsible for the unique functions of the inner BRB. Branched chain amino transferase (BCAT) is involved in de novo glutamate synthesis by transferring nitrogen from the branched-chain amino acids to α -ketoglutarate and vice versa primarily in the retina and the brain [26]. BCATc is proposed to play a more important role in de novo glutamate synthesis at the inner BRB than the BBB. This was supported by the finding that the percentages of glutamate input into the glutamate/glutamine cycle, which are provided by de novo glutamate synthesis, are about 30% and 20% in the retina and whole brain, respectively [26]. Further studies are needed to understand these functions in the retina in vivo. It is important to investigate whether other clones with an expression ratio between 2 and 5 (clones 5, 6, 7, and 8) reflect differences in the two tissues. This confirms that mRNA differential display analysis using both cell lines is a useful technique to determine differences in gene expression between the inner BRB and BBB.

In conclusion, eight clones were identified as highly expressed genes in TR-iBRB cells compared with TR-BBB cells using mRNA differential display analysis. Of these eight clones, M-cadherin, GATA-3, and BCATc were more abundantly expressed in TR-iBRB cells than TR-BBB cells and may indeed be involved in unique functions at the inner BRB. Moreover, rat M-cadherin gene, which has been cloned from TR-iBRB cells, for the first time, was expressed to a much greater extent in TR-iBRB than in TR-BBB and may be responsible for some cell-cell adhesion differences between the two tissues. The selective expression of genes at the inner BRB compared with the BBB may have important implications for the unique function of the inner BRB and the retina.

ACKNOWLEDGEMENTS

The authors thank Drs. Tadahiro Oshida, Hideaki Takeuchi, and Gozo Tsujimoto for valuable discussions. This study was supported, in part, by a Grant in Aid for Scientific Research from the Japan Society for the Promotion of Science.

REFERENCES

1. Stewart PA, Tuor UI. Blood-eye barriers in the rat: correlation of ultrastructure with function. *J Comp Neurol* 1994; 340:566-76.
2. Holash JA, Stewart PA. The relationship of astrocyte-like cells to the vessels that contribute to the blood-ocular barriers. *Brain Res* 1993; 629:218-24.
3. Takata K, Kasahara T, Kasahara M, Ezaki O, Iitirano II. Ultracytochemical localization of the erythrocyte/HepG2-type glucose transporter (GLUT1) in cells of the blood-retinal barrier in the rat. *Invest Ophthalmol Vis Sci* 1992; 33:377-83.
4. Nakashima T, Tomi M, Katayama K, Tachikawa M, Watanabe M, Terasaki T, Hosoya K. Blood-to-retina transport of creatine via creatine transporter (CRT) at the rat inner blood-retinal barrier. *J Neurochem* 2004; 89:1454-61.
5. Ohtsuki S, Tachikawa M, Takanaga H, Shimizu H, Watanabe M, Hosoya K, Terasaki T. The blood-brain barrier creatine transporter is a major pathway for supplying creatine to the brain. *J Cereb Blood Flow Metab* 2002; 22:1327-35.
6. Pardridge WM, Boado RJ, Farrell CR. Brain-type glucose transporter (GLUT-1) is selectively localized to the blood-brain barrier. Studies with quantitative western blotting and in situ hybridization. *J Biol Chem* 1990; 265:18035-40.
7. Schinkel AH, Smit JJ, van Tellingen O, Beijnen JH, Wagenaar E, van Deemter L, Mol CA, van der Valk MA, Robanus-Maandag EC, te Riele HP, Biersma AJ, Borst P. Disruption of the mouse mdr1a P-glycoprotein gene leads to a deficiency in the blood-brain barrier and to increased sensitivity to drugs. *Cell* 1994; 77:491-502.
8. Hosoya K, Saeki S, Terasaki T. Activation of carrier-mediated transport of L-cystine at the blood-brain and blood-retinal barriers in vivo. *Microvasc Res* 2001; 62:136-42.
9. Hosoya KI, Takashima T, Tetsuka K, Nagura T, Ohtsuki S, Takanaga H, Ueda M, Yanai N, Obinata M, Terasaki T. mRNA expression and transport characterization of conditionally immortalized rat brain capillary endothelial cell lines; a new in vitro BBB model for drug targeting. *J Drug Target* 2000; 8:357-70.
10. Hosoya K, Tomi M, Ohtsuki S, Takanaga H, Ueda M, Yanai N, Obinata M, Terasaki T. Conditionally immortalized retinal capillary endothelial cell lines (TR-iBRB) expressing differentiated endothelial cell functions derived from a transgenic rat. *Exp Eye Res* 2001; 72:163-72.
11. Terasaki T, Ohtsuki S, Hori S, Takanaga H, Nakashima F, Hosoya K. New approaches to in vitro models of blood-brain barrier drug transport. *Drug Discov Today* 2003; 8:944-54.
12. Donalies M, Cramer M, Ringwald M, Starzinski-Powitz A. Expression of M-cadherin, a member of the cadherin multigene family, correlates with differentiation of skeletal muscle cells. *Proc Natl Acad Sci U S A* 1991; 88:8024-8.
13. Shimoyama Y, Shibata T, Kitajima M, Hirohashi S. Molecular cloning and characterization of a novel human classic cadherin homologous with mouse muscle cadherin. *J Biol Chem* 1998; 273:10011-8.
14. Zeschnick M, Kozian D, Kuch C, Schmoll M, Starzinski-Powitz A. Involvement of M-cadherin in terminal differentiation of skeletal muscle cells. *J Cell Sci* 1995; 108:2973-81.
15. Guimaraes MJ, Lee F, Zlotnik A, McClanahan T. Differential display by PCR: novel findings and applications. *Nucleic Acids Res* 1995; 23:1832-3.
16. Nollet F, Kools P, van Roy F. Phylogenetic analysis of the cadherin superfamily allows identification of six major subfamilies besides several solitary members. *J Mol Biol* 2000; 299:551-72.
17. Vittet D, Buchou T, Schweitzer A, Dejana E, Huber P. Targeted null-mutation in the vascular endothelial-cadherin gene impairs the organization of vascular-like structures in embryoid bodies. *Proc Natl Acad Sci U S A* 1997; 94:6273-8.
18. Breier G, Breviaro F, Caveda L, Berthier R, Schnurch H, Gotsch

- U, Vestweber D, Risau W, Dejana E. Molecular cloning and expression of murine vascular endothelial-cadherin in early stage development of cardiovascular system. *Blood* 1996; 87:630-41.
19. Russ PK, Davidson MK, Hoffman LII, Haselton FR. Partial characterization of the human retinal endothelial cell tight and adherens junction complexes. *Invest Ophthalmol Vis Sci* 1998; 39:2479-85.
20. Gerhardt H, Liebner S, Redies C, Wolburg H. N-cadherin expression in endothelial cells during early angiogenesis in the eye and brain of the chicken: relation to blood-retina and blood-brain barrier development. *Eur J Neurosci* 1999; 11:1191-201.
21. Hollnagel A, Grund C, Franke WW, Arnold HH. The cell adhesion molecule M-cadherin is not essential for muscle development and regeneration. *Mol Cell Biol* 2002; 22:4760-70.
22. Kern TS, Engerman RL. Capillary lesions develop in retina rather than cerebral cortex in diabetes and experimental galactosemia. *Arch Ophthalmol* 1996; 114:306-10.
23. Nielsen H, Engelbrecht J, Brunak S, von Heijne G. Identification of prokaryotic and eukaryotic signal peptides and prediction of their cleavage sites. *Protein Eng* 1997; 10:1-6.
24. Overduin M, Harvey TS, Bagby S, Tong KI, Yau P, Takeichi M, Ikura M. Solution structure of the epithelial cadherin domain responsible for selective cell adhesion. *Science* 1995; 267:386-9.
25. Pai SY, Truitt ML, Ho IC. GATA-3 deficiency abrogates the development and maintenance of T helper type 2 cells. *Proc Natl Acad Sci U S A* 2004; 101:1993-8.
26. Lieth E, LaNoue KF, Berkich DA, Xu B, Ratz M, Taylor C, Hutson SM. Nitrogen shuttling between neurons and glial cells during glutamate synthesis. *J Neurochem* 2001; 76:1712-23.

The print version of this article was created on 9 Aug 2004. This reflects all typographical corrections and errata to the article through that date. Details of any changes may be found in the online version of the article.

Downregulation of retinal GLUT1 in diabetes by ubiquitinylation

Rosa Fernandes,^{1,2} Ana Luisa Carvalho,³ Arno Kumagai,² Raquel Seica,⁴ Ken-ichi Hosoya,⁵ Tetsuya Terasaki,⁶ Joaquim Murta,¹ Paulo Pereira,¹ Carlos Faro⁷

¹Biomedical Institute for Research in Light and Image, Center of Ophthalmology, University of Coimbra, Coimbra, Portugal; ²Department of Internal Medicine and the Juvenile Diabetes Research Foundation (JRF) Center for Complications in Diabetes, University of Michigan Medical School, Ann Arbor, MI; ³Department of Zoology, ⁴Faculty of Medicine, and ⁵Department of Biochemistry, Center for Neuroscience, University of Coimbra, Coimbra, Portugal; ⁶Faculty of Pharmaceutical Sciences, Toyama Medical and Pharmaceutical University, 2630 Sugitani, Toyama, Japan; ⁷Graduate School of Pharmaceutical Sciences, Tohoku University, Aoba, Aramaki, Aoba-ku, Sendai, Japan

Purpose: To investigate the effect of chronic hyperglycemia on the levels of the glucose transporter GLUT1 in retina and its ubiquitinylation.

Methods: Two diabetic animal models (Goto Kakizaki rats and alloxan-induced diabetic rabbits) and retinal endothelial cells in culture were used. GLUT1 content was determined by western blotting. GLUT1 mRNA was determined by RT-PCR and northern blotting. Ubiquitin conjugates were evaluated by western blot analysis. In vitro ubiquitin conjugation activity was evaluated in supernatants using radiolabeled ubiquitin. Evidence for GLUT1 ubiquitinylation was further investigated by transfecting IIEK293 cells with a hemagglutinin (HIA)-tagged ubiquitin cDNA followed by immunoprecipitation of the cell lysates.

Results: Chronic hyperglycemia resulted in a significant decrease on the amount of GLUT1 protein without significant changes on the GLUT1 mRNA in the retinas of diabetic GK rats and alloxan treated rabbits, and in high glucose treated retinal endothelial cells, compared to controls. The content of high molecular weight ubiquitin conjugates was higher both in the membrane fractions of diabetic retinas and in endothelial cells incubated with high glucose concentrations. GLUT1 immunoprecipitated from diabetic retinas crossreacted with antibodies directed against ubiquitin suggesting that GLUT1 is posttranslationally modified by monoubiquitinylation. Cells transfected with HIA-tagged ubiquitin revealed crossreactivity with anti-GLUT1 antibodies on the HA immunoprecipitates.

Conclusions: The data indicate that retinal GLUT1 abundance decreases in experimental diabetes and with exposure of retinal endothelial cells to elevated glucose concentrations. Results further suggest that decreased abundance of GLUT1 may be associated with its increased degradation by a ubiquitin dependent mechanism. Ubiquitinylation of GLUT1 may be the mechanism targeting GLUT1 for degradation in diabetes.

Hyperglycemia is considered the major determinant of vascular complications and development of diabetic retinopathy. The molecular mechanisms underlying such changes are poorly understood. Nevertheless, there are some pathways proposed to be involved in glucose toxicity, including nonenzymatic glycation, activation of protein kinase C, and increased production of reactive oxygen species combined with impaired antioxidative defenses [1,2]. In addition to nutrient supply, the capillaries of the retina constitute a barrier to the passage of blood-borne compounds and solutes between the blood and the retina. In the inner retina, this barrier is comprised of microvascular endothelial cells and is known as the inner blood-retinal barrier (BRB). The outer retina possesses another barrier, the outer BRB, that consists of the retinal pigment epithelial cells. Due to the presence of the BRB, glucose cannot freely pass from blood to the retina. Glucose transport across this barrier is mediated by a facilitative transporter, GLUT1 [3].

The regulation of GLUT1 in retinal endothelial cells in response to chronic hyperglycemia is not clear. There are conflicting data concerning the effect of hyperglycemia on glucose transport and on GLUT1 expression. In a diabetic animal model, Badr and colleagues showed a decrease of approximately 50% in whole retinal GLUT1 and retinal microvascular GLUT1, for 8 week-long diabetes [4]. Mandarino et al [5] reported an unchanged uptake of 3-O-methylglucose (3-OMG) in high glucose treated bovine retinal endothelial cells compared with pericytes, which showed a downregulation in 3-OMG uptake. In contrast, very recently, Busik et al [6] showed an increase of glucose uptake in human retinal vascular endothelial cells incubated under high glucose, without a change in endothelial cell GLUT1.

The effect of diabetes on expression and regulation of the GLUT1 glucose transporter in endothelial cells is evaluated in this study. To investigate the regulation of GLUT1 levels in BRB in response to hyperglycemia, we used two diabetic animal models and retinal endothelial cells. We demonstrate that GLUT1 conjugation with ubiquitin may constitute a posttranslational mechanism through which the cellular levels of GLUT1 are regulated under hyperglycemia.

Correspondence to: Paulo Pereira, Department of Ophthalmology, IBILI Azinhaga de Santa Comba, Celas, 3000-354, Portugal; Phone: (351) 239480225; FAX: (351) 239480280; email: ppereira@imagem.ibili.uc.pt

METHODS

Animals: In this study two diabetic animal models were used, the Goto Kakizaki (GK) rats and the alloxan-induced diabetic rabbits. Wistar and GK rats were obtained from a local breeding colony maintained at the University Hospitals of Coimbra. After 6 weeks of age, the GK rats showed persistent hyperglycemia. Six month old and one year old diabetic and age matched nondiabetic Wistar control rats were used in these experiments. The rats were fed normal rat chow ad libitum and maintained in temperature-controlled facilities with 12 h light-dark cycles. Glucose concentrations were measured on tail blood samples using a glucose monitor (Gluco Touch; Lifescan, Milpitas, CA).

Diabetes in rabbits was induced by the injection of a freshly prepared solution of alloxan in serum at a dose of 110 mg/kg body in a prominent ear vein. A sample of blood was obtained weekly from the ear vein to monitor glucose concentrations.

All animals were handled in accordance with ARVO Statement for the use of Animals in Ophthalmic and Vision Research.

Rats and rabbits were sacrificed by decapitation and their eyes were quickly removed. Retinas were isolated and wrapped in aluminum foil, frozen on liquid nitrogen and stored at -80 °C until used.

Primary cell cultures of bovine retinal endothelial cells: Bovine retinas were the source of capillaries used to isolate cells for primary culture. Cow eyes were obtained from a local abattoir. Primary bovine retinal endothelial cells (BREC) cultures were established from fresh calf eyes. Under sterile conditions, the retinas were isolated and washed in Dulbecco's modified Eagle's medium (DMEM; Invitrogen, Carlsbad, CA) and pieces of adherent retinal pigment epithelial cells were removed. The retinas were transferred to an enzyme solution containing pronase (100 µg/ml; Roche, Mannheim, Germany), collagenase (500 µg/ml; Invitrogen) and DNase (70 µg/ml; Sigma-Aldrich, St. Louis, MO) and incubated with shaking at 37 °C for 20 min. After incubation, the retinal digest was passed through 210 and 50 µm nylon mesh and the microvessels trapped on top of the 50 µm mesh were collected in DMEM

by centrifugation. The fragments were resuspended in DMEM with 15% fetal calf serum (FCS), 20 µg/ml endothelial growth supplement (Roche, Mannheim, Germany), heparin (100 µg/ml) and antibiotic-antimycotic solution (Sigma, St. Louis, MO), plated and grown on fibronectin coated dishes in low glucose DMEM, at 37 °C with 5% CO₂.

To determine the effect of high glucose on GLUT1 expression, BREC were grown in low (5.5 mM) or high (25 mM) D-glucose medium up to 48 h.

Cell line of retinal capillary endothelial cells: A conditionally immortalized retinal capillary endothelial cell line (TR-iBRB) [7] was grown and maintained in DMEM with low glucose, containing 10% fetal bovine serum (FBS; Gibco BRL Life Technologies, Inchiman, UK), 100 U/ml penicillin G, 100 U/ml streptomycin (Sigma), in a humidified atmosphere composed of 95% air and 5% CO₂ at 33 °C. Cells were grown to approximately 40-50% confluence and incubated in regular DMEM containing 5.5 or 25 mM glucose at 37 °C. Control experiments using mannitol were performed to test the effect of high osmolarity on the GLUT1 expression. There were no changes in the GLUT1 expression in cells treated with 25 mM mannitol for 48 h.

Human embryonic kidney (HEK)293 cells were cultured in DMEM supplemented with 10% FBS, 100 U/ml penicillin G, 100 U/ml streptomycin, in a humidified atmosphere composed of 95% air and 5% CO₂ at 37 °C.

Antibodies: Goat polyclonal antibody raised against the COOH terminus of rabbit GLUT1 was purchased from Santa Cruz Biotechnology, Inc. (Santa Cruz, California). Rabbit polyclonal antibody raised against purified human erythrocyte GLUT1 was a kind gift from Christin Carter-Su. Monoclonal anti-ubiquitin antibody was purchased from Affiniti Research Products Ltd. (Mamhead Castle, UK) and polyclonal anti-ubiquitin antibody was a kind gift from Dr. Fu Shang (Tufts University, Boston, MA). Mouse monoclonal antibody against actin was purchased from Boehringer Mannheim (Mannheim, Germany). Polyclonal anti-hemagglutinin antibody was purchased from Zymed Laboratories Inc. (South San Francisco, CA).

TABLE 1. BODY WEIGHT AND PLASMA GLUCOSE LEVELS FOR CONTROL (WISTAR) AND DIABETIC (GK) RATS

	n	Body weight (g)	Serum glucose (mg/dL)
Wistar rats			
6 months	5	552±40	121± 6
12 months	4	811±42	91± 7
GK rats			
6 months	4	367±14*	267±34*
12 months	4	423±52*	329±25*

Values in table are means±standard error. An asterisk (*) indicates a statistically significant difference (p<0.01) between diabetic (GK) and age matched control (Wistar) rats.

TABLE 2. BODY WEIGHT AND PLASMA GLUCOSE LEVELS FOR NONDIABETIC AND DIABETIC RABBITS

	n	Body weight (g)	Serum glucose (mg/dL)
Control			
	5	2420± 79	102± 3
Diabetic			
2 weeks	6	2575± 80	365±39
2 months	7	3097±198	378±48
4 months	7	3668± 95	332±27

Values in table are means±standard error. There were statistically significant differences (p<0.01) for measurements of body weight and serum glucose between diabetic (alloxan-induced) rabbits and control rabbits.

Isolation of the membrane fraction from the retina of diabetic and control animals: Total retina homogenates from diabetic or control animals were obtained by tissue lysis in 10 mM Tris-HCl, 1 mM EDTA, 250 mM sucrose, protease inhibitors, pH 7.4, at 4 °C and mechanical disruption using a Potter-Elvehjem homogenizer (50-60 strokes). The samples were centrifuged at 900x g to remove nuclei, mitochondria and unlysed cells, and re-centrifuged at 100,000x g for 75 min to obtain the total cell membranes. The membrane pellet was resuspended in 10 mM Tris-HCl, 1 mM EDTA, pH 7.4 containing protease inhibitors, 0.5% sodium deoxycholate (DOC) and 1% TritonX-100. The samples were then centrifuged at

14,000x g to remove the insoluble fraction. The protein concentration was measured using the BCA reagent (Pierce, Rockford, IL) with BSA as the standard.

Extracts from retinal endothelial cells (BREC and TR-iBRB cells): After incubation with glucose, the BREC and TR-iBRB cells were washed twice with ice-cold PBS and then lysed with 10 mM Tris-HCl, 1 mM EDTA, pH 7.4 containing protease inhibitors, 0.5% DOC and 1% Triton X-100. The lysates were sonicated 6 times for 3 s and then centrifuged at 14,000x g for 15 min. The supernatants were used to determine the protein concentration and were then denatured with Laemmli buffer.

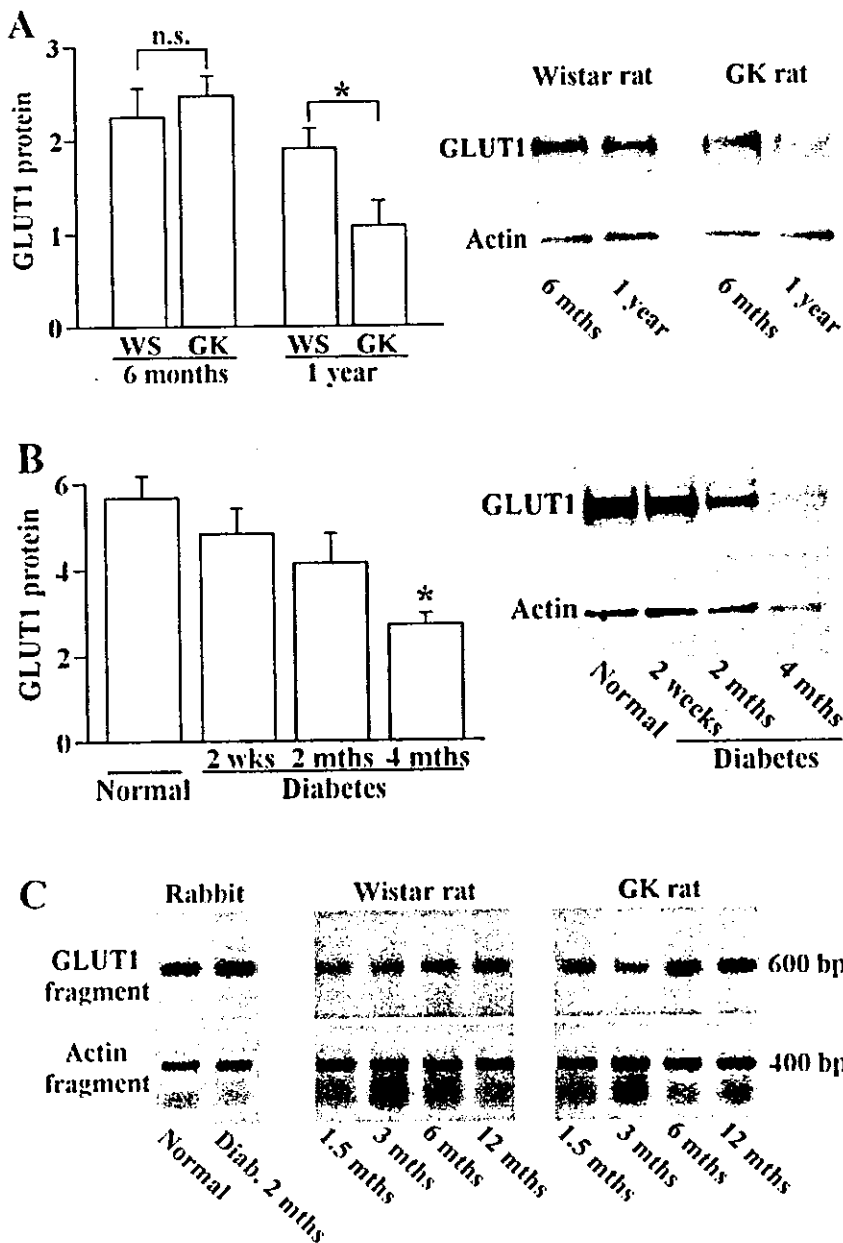


Figure 1. Effect of diabetes on GLUT1 expression in retina. A: GLUT1 protein expression in retina from 1 year old non-diabetic rats is greater than in age matched diabetic GK rats. Membrane fractions were isolated from rat retinas. Equal amounts of protein (30 µg) were subjected to immunoblotting and membranes were probed with anti-GLUT1 antibodies. Actin expression on the same membrane is included to demonstrate comparable loading of lanes. Graphical summary and western blots are provided. Bars represent standard errors (4 rats/group). The asterisk (*) indicates that the GLUT1 protein expression for 1 year old diabetic GK rats are statically different from the age matched control Wistar rats ($p < 0.05$). B: GLUT1 protein expression in diabetic rabbit retinas is decreased compared to controls. The duration of diabetes was 2 weeks, 2 and 4 months. Membrane fractions were isolated from rabbit retinas. Equal amounts of protein (5 µg) were subjected to immunoblotting and probed with antibodies directed against GLUT1 and actin. Western blots are provided. The graphic represents the results normalized for actin. Bars represent standard errors (5 rabbits/group). The asterisk (*) indicates that the GLUT1 protein expression for rabbits with diabetes for 4 months are significantly different from the the control rabbits ($p < 0.01$). C: Slight increase on retinal GLUT1 mRNA levels in diabetic animals. Total retinal RNA (1 µg or 150 ng) was subjected to RT-PCR analysis for determination of GLUT1 and actin mRNA levels.

Isolation of total RNA from retina and TR-iBRB cells: Total RNA was isolated from rat and rabbit retinas using TRIzol® Reagent (Gibco BRL, Paisley, UK), according to manufacturer's protocol. Briefly, tissues were homogenized in guanidium isothiocyanate and phenol. Chloroform extraction allowed recovery of RNA in the aqueous phase. The RNA was then precipitated with isopropyl alcohol, and the RNA pellet was washed with 75% ethanol and redissolved in DEPC treated water. Total RNA samples were treated with RNase-free DNase prior to reverse transcription to ensure that the samples were free of contaminating DNA.

Total RNA from TR-iBRB cells was isolated using the RNeasy mini kit (Qiagen, Valencia, CA) according to the manufacturer's protocol.

The total amount of RNA was quantified by optical density (OD) measurements at 260 nm and the purity was evaluated by measuring ratio of OD at 260 and 280 nm.

Western blotting: For the western blot analysis, 5 to 30 µg protein were loaded per lane on sodium dodecyl sulphate-polyacrylamide gels (SDS-PAGE). Following electrophoresis and transfer to polyvinylidene fluoride (PVDF) membranes (Boehringer Mannheim), the blots were incubated in Tris buffered saline (20 mM Tris, 137 mM NaCl, pH 7.6) containing 0.1% Tween 20 (TBST), and 5% nonfat milk for 1 h. Membranes were then incubated with 1:1,000 dilution of affinity-purified goat polyclonal anti-GLUT1 (Santa Cruz Biotechnology, Inc.), 1:10,000 dilution of rabbit polyclonal antibody against GLUT1, 1:10,000 dilution of the anti-actin antibody, or 1:1,000 dilution of mouse monoclonal (FK2) or polyclonal antibodies to ubiquitinated proteins, for 1 h 30 min, in TBST containing 0.5% non fat milk. After five washes with TBST, blots were reacted for 1 h with 1:10,000 dilution of secondary antibodies coupled to alkaline-phosphatase in TBST containing 0.5% nonfat milk, and were then washed 5 times with TBST and were developed using an enhanced fluorescence kit (Amersham Pharmacia Biotech, Buckinghamshire, UK). Blots were scanned in the Storm 860 (Molecular Dynamics, Amersham Biosciences, Uppsala, Sweden) and the optical density of the bands was measured with Image Quant 5.0 Software (Molecular Dynamics). The intensity of the GLUT1

bands was normalized for every sample relatively to the intensity of the respective actin bands.

Determination of ubiquitin conjugating activity: The ability of TR-iBRB or retina supernatants to catalyse the conjugation of exogenous radiolabeled ubiquitin (¹²⁵I) to endogenous proteins was determined using an assay modified from Hershko et al [8]. Briefly, cells or retinas were sonicated in 50 mM Tris-HCl buffer, pH 7.6. The lysates were centrifuged at 14,000x g during 10 min, at 4 °C. Reactions were performed in a final volume of 25 µl, containing 15 µl of supernatant (80 µg of TR-iBRB cell supernatant lysates or 50 µg of retina supernatant lysates), 10 µl of conjugation buffer solution (50 mM Tris-HCl, pH 7.6, 5 mM MgCl₂, 1 mM DTT, 2 mM ATP, 34.8 U/ml creatine phosphokinase, 10 mM creatine phosphate) and 0.3 µg of ¹²⁵I-ubiquitin (approximately 2 x 10⁵ c.p.m.). Controls were generated by incubation with buffer A (50 mM Tris-HCl, pH 7.6, 5 mM MgCl₂ and 1 mM DTT). After 20 min of incubation at 37 °C, the reaction was terminated by the addition of 25 µl of 2X Laemmli buffer followed by at least 30 min at room temperature. Aliquots of the assays were separated by SDS/12%-PAGE. Autoradiograms of dried gels were obtained and scanned for densitometric analysis.

Northern blotting: Total RNA was isolated from control and high glucose treated TR-iBRB cells. Aliquots (20 µg) of total RNA were loaded on a 2 M formaldehyde 1% agarose gel, and run overnight at 20 V. RNA was then transferred to a nylon membrane (Schleicher & Schuell BioScience, Inc., Keene, NH) by capillary action for about 24 h. Northern blot analysis for GLUT1 and mouse actin were performed as previously described [9], using a 512 kb *Pst*I fragment of the bovine blood-brain barrier glucose transporter cDNA [10] linearized with *Hind*III, and a mouse actin clone, pAM-91 (generously provided by Michael J. Getz, Mayo Clinic/Foundation, Rochester, MI), linearized with *Eco*RI. Both cDNAs were labeled with [³²P]-dCTP using a random primer method, as described previously [9]. Quantification of autoradiograms was performed using NIH Image software (version 1.6) and the GLUT1 signal was normalized against the signal for actin.

Semi quantitative RT-PCR analyses: GLUT1 mRNA levels were determined by quantitative reverse transcription-PCR

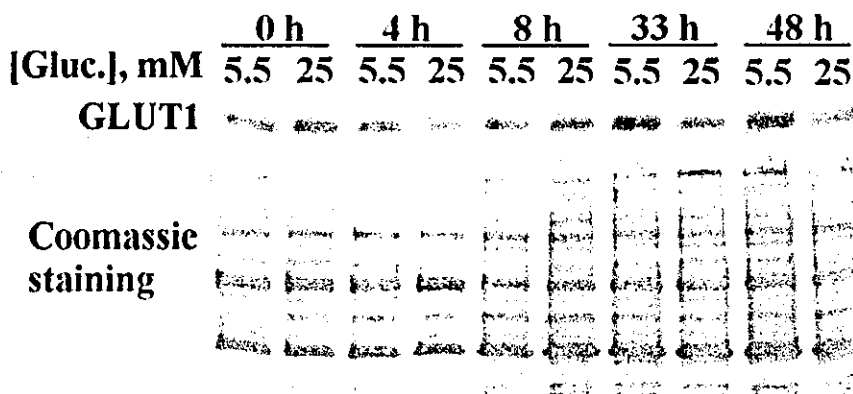


Figure 2. Effect of high glucose on GLUT1 expression in primary cultures of BREC cells. In BREC cells exposed to high glucose concentration there is a decrease in the amount of GLUT1 protein. The cells were solubilized in Laemmli buffer without β -Mercaptoethanol and equal amounts of protein (30 µg) were loaded on a 12% polyacrylamide gel following addition of reducing agent β -Mercaptoethanol. The proteins were resolved by SDS-PAGE, transferred to PVDF membrane and probed with an antiserum against GLUT1. Coomassie staining is used as a control for total protein loading.

of total RNA from retinas, using the forward primer 5'-CTC CAC GAG CAT CTT CGA GAA G-3' and the reverse primer 5'-TCA CAC TTG GGA ATC AGC CC-3' for amplification of GLUT1, and the forward primer 5'-GAC TAC CTC ATG AAG ATC CT-3' and the reverse primer 5'-ATC TTG ATC TTC ATG GTG CTG-3' for amplification of actin.

For the RT-PCR reactions, 150 ng or 1 µg of total RNA from rabbits and rats retinas, respectively, were used for GLUT1 and actin amplification. Amplification products were electrophoresed on 1% agarose gels and stained with ethidium bromide. The gel was then photographed on a UV transilluminator.

Transfection: HEK293 cells were transiently transfected with the plasmid encoding hemagglutinin-tagged ubiquitin, under the control of the CMV promoter, which was kindly donated by Dr. Bohmann, University of Rochester, Rochester, NY. The transfection was carried out using LipofectAMINE™ (Gibco BRL). Cells were incubated with plasmid DNA for 6 h, and the same volume of fresh medium, containing 10% FBS, was then added to the cells. Cells were used 24 h after transfection.

Immunoprecipitation: Immunoprecipitations were performed by incubation of the protein extracts from retinas or cells with the anti-GLUT1 (2.5 µg) or anti-HA (3.75 µg) antibodies, overnight at 4 °C. The protein-antibodies complexes were collected on protein G-Sepharose or protein A-Sepharose beads. The beads were extensively washed and the immuno-

precipitated proteins were eluted in Laemmli buffer and resolved by SDS-PAGE.

Statistical analysis: Measurements of the GLUT1 expression levels were averaged for each group of animals. A minimum of three northern blot analysis was done for each group of animals and a minimum of four measurements of GLUT1 protein expression by western blot analysis was performed. The mean values from each group were then used to compute an overall mean and standard error of the mean. Comparisons between groups were made with an unpaired two tailed Student's t-test. The α level for statistical significance was set at 0.05.

RESULTS

Animal and cell models of diabetes: To establish the effect of hyperglycemia on the expression of GLUT1, the level of GLUT1 was analysed in two diabetic animal models and compared to the level of expression of GLUT1 in control animals.

One of the diabetic animal models used was the GK rat, which spontaneously develops non-insulin-dependent type 2 diabetes. These animals begin to develop chronic hyperglycemia at 4 to 6 weeks of age [11] which remains stable during ageing of the animals. Associated with hyperglycemia, these animals present hyperinsulinemia, glucose intolerance and some of the metabolic and anatomic changes similar to those observed in human diabetic retinopathy [12-14]. The GK rats were produced by selective breeding of normal Wistar rats

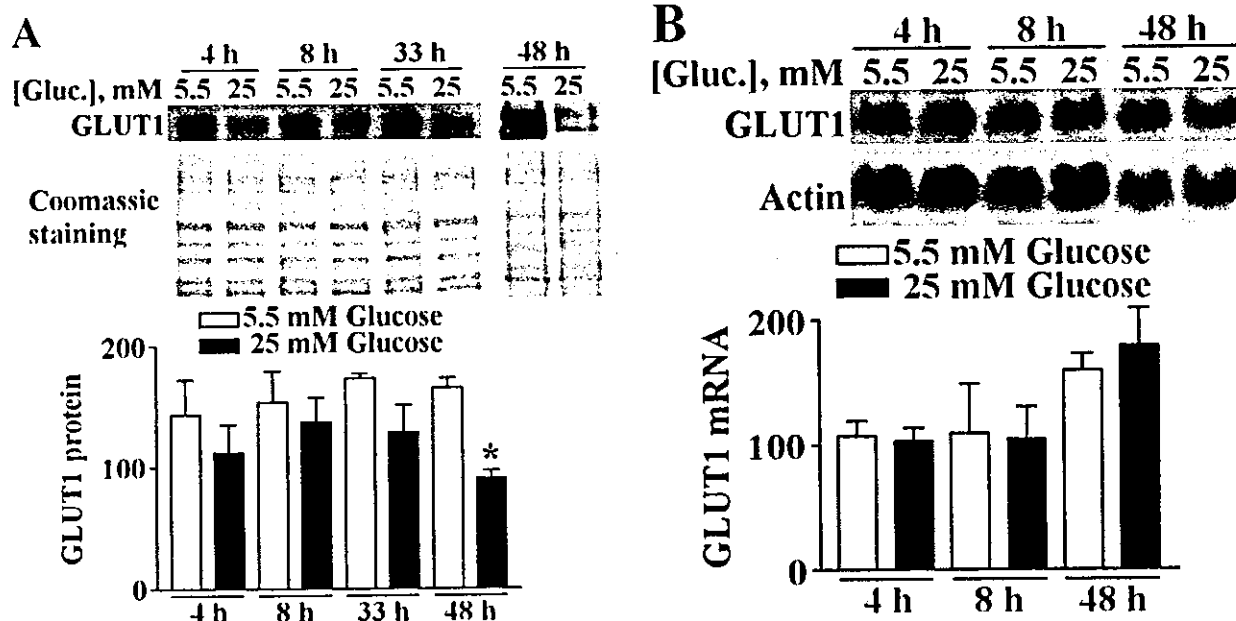


Figure 3. Effect of high glucose on expression of GLUT1 in TR-iBRB cells. A: In TR-iBRB cells exposed to high glucose concentration there is a subnormal expression of GLUT1 protein. The cells were solubilized in SDS-PAGE buffer and equal amounts of protein (30 µg) were loaded on a 12% polyacrylamide gel. The proteins were resolved by SDS-PAGE, transferred to PVDF membrane and probed with an antiserum against GLUT1. Bars represent standard errors (3 rats/group). The asterisk (*) indicates p<0.05. B: There are no significant changes in the levels of GLUT1 mRNA after 48 h of hyperglycemia. The total RNA was isolated from control and high glucose treated TR-iBRB cells and northern blot analysis was performed. Bars represent standard errors (3 rats/group).

and therefore the Wistar rats are considered appropriate controls since these two groups of animals have the same genetic background [11,15]. The second diabetic animal model used was the alloxan treated rabbit that mimics *type 1* diabetes.

Several reports showed retinal abnormalities such as microaneurysms, pericyte loss, acellular capillaries [16] and ultrastructural disorders of vessels and basement membrane [17] in alloxan-induced diabetes.

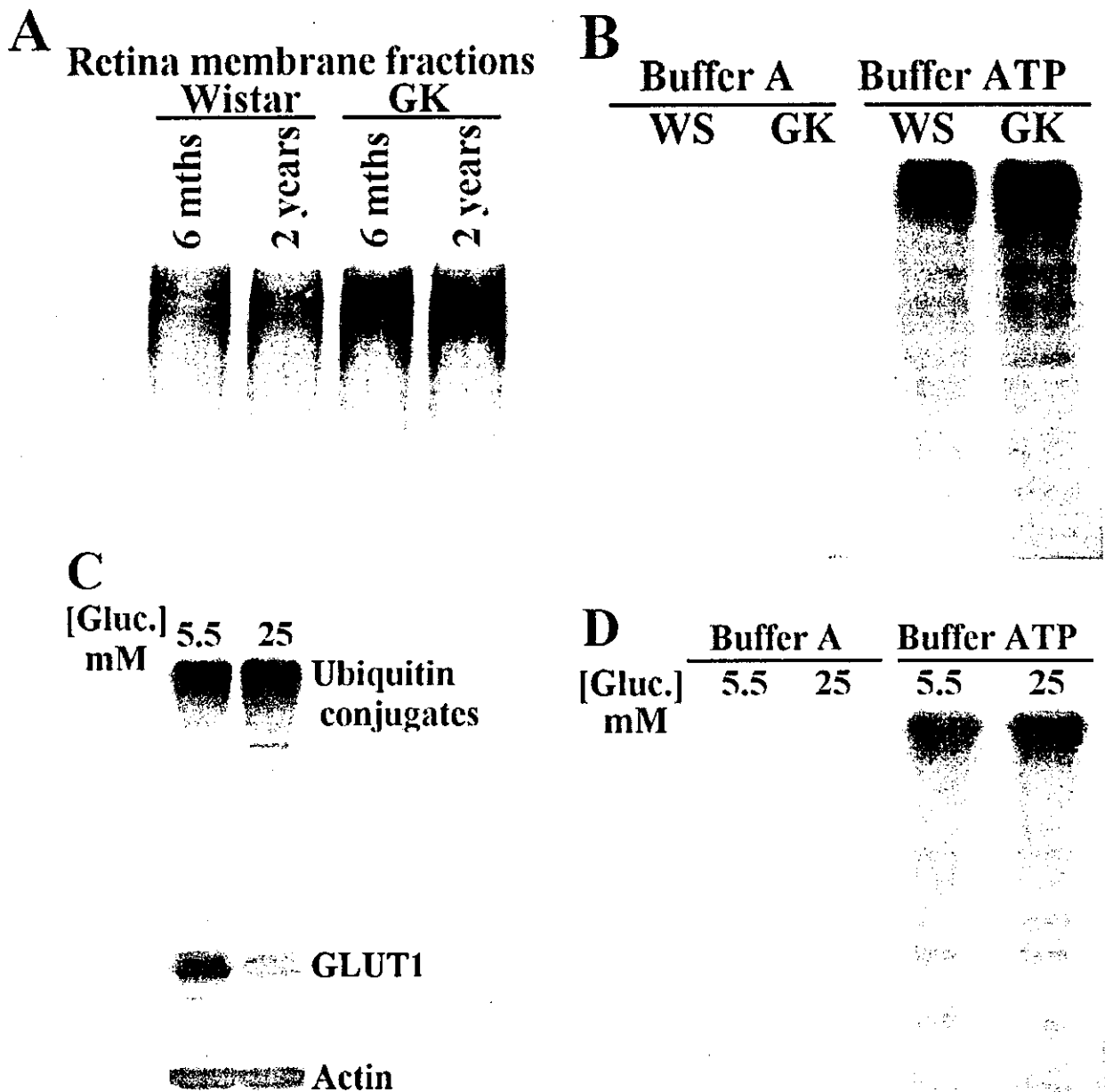


Figure 4. Effect of hyperglycemia on ubiquitinylation. Hyperglycemia altered endogenous ubiquitin conjugates and de novo ubiquitin conjugation activity in diabetic animal (A, B) and in cells exposed to high glucose (C, D). Diabetic animals (A, lanes labeled "GK") or cells exposed to high glucose (C, right) show increased levels of endogenous high molecular weight ubiquitin conjugates. Cells exposed to high glucose also show a significant decrease in the total amount of GLUT1 (C). Retinal tissues or cells were lysed, proteins were separated by SDS-PAGE, transferred to PVDF membranes and probed with antibodies directed against ubiquitin conjugates (FK2). The increase in endogenous ubiquitin conjugates is associated with an increased ability of retinal (B) or cell (D) extracts to conjugate radiolabeled ¹²⁵I-ubiquitin to endogenous substrates. Conjugation activity was determined either in the presence of an ATP generating buffer ("Buffer ATP" in B and D) or as a control in the absence of ATP ("Buffer A" in B and D). Conjugation experiments were performed for 20 min. Proteins were resolved by SDS-PAGE and the dried gels were used for autoradiography.

The average blood glucose concentrations and body weight for the 6 months and 1 year old diabetic GK rats and age matched Wistar rats are provided in Table 1. Data on diabetic rabbits and healthy controls are provided in Table 2. Diabetic rats were hyperglycemic and they failed to gain weight at a normal rate. The average blood glucose concentrations for diabetic rats and rabbits was significantly higher ($p < 0.01$) than that of control animals.

For this study, two retinal endothelial cell models were used. A first approach to the effect of hyperglycemia on GLUT1 levels used primary cultures of endothelial cells obtained from bovine retinas. Once glucose-related changes were established in primary cultures, a cell line was used. TR-iBRB is a conditionally immortalized retinal capillary endothelial cell line. The cells present a doubling time of 19-21 h and exhibit the properties of retinal capillary endothelial cells [7]. To mimic the diabetic condition, both cell types were exposed to high glucose.

Diabetic animals present lower levels of GLUT1 in retina:

To study the effect of chronic hyperglycemia on GLUT1 expression, we analysed the GLUT1 content in membrane fractions isolated from the whole retinas of diabetic and control animals (Figure 1). As a loading control, membranes were probed with anti-actin antibody. At the age of 6 weeks before GK rats developed diabetes, the Wistar and GK rats showed comparable levels of GLUT1 and endogenous ubiquitin conjugates, thus indicating that the results obtained for older animals are not due to differences in the genetic background of these animals (data not shown). Data presented in Figure 1A indicate that there are no significant changes on GLUT1 protein levels between 6 months old WS rats (2.1 ± 0.40) and GK rats (2.2 ± 0.30). For both control and diabetic rats, an age related decrease on the content of GLUT1 protein was observed. However, GLUT1 expression was significantly lower in of 1 year old GK rats (1.2 ± 0.33) as compared to the age matched WS rats (1.7 ± 0.28), $p < 0.05$ level (Figure 1A).

A similar situation is observed in alloxan-induced diabetic rabbits. GLUT1 protein in the retina of non-diabetic rabbits is greater than that in diabetic rabbits (Figure 1B). Since no age-related changes were observed in normal rabbits (data not shown), only one time point was considered in Figure 1B for control animals. To confirm that equal amounts of protein were loaded on each lane, the membranes were stripped and reprobed for actin. Diabetic animals with a duration of disease of 4 months presented a 50% decrease on the amount of the glucose transporter in the retina (control rabbits: 5.7 ± 0.50 and diabetic rabbits: 2.7 ± 0.25 ; $p < 0.01$).

The levels of GLUT1 mRNA were determined by RT-PCR. Total RNA was isolated from whole retinas from rabbits and rats and GLUT1 was amplified by RT-PCR (Figure 1C). β -actin was amplified to confirm that equal quantities of RNA were used for the amplification. There is no evidence for a decrease on mRNA for GLUT1; therefore, the lower levels of protein are probably the result of an increased degradation of GLUT1 associated with diabetes.

High glucose results in a decrease in GLUT1 in retinal endothelial cells: As a first approach to study GLUT1 ex-

pression upon hyperglycemia, we used primary retinal endothelial cells in culture. BREC were incubated in the presence of low (5.5 mM) and high (25 mM) glucose up to 48 h and cells were then lysed and protein separated by SDS-PAGE, transferred to PVDF membranes and probed with antibodies against GLUT1 (Figure 2). After 48 h of incubation with high glucose, there is a decrease of approximately 35% in the

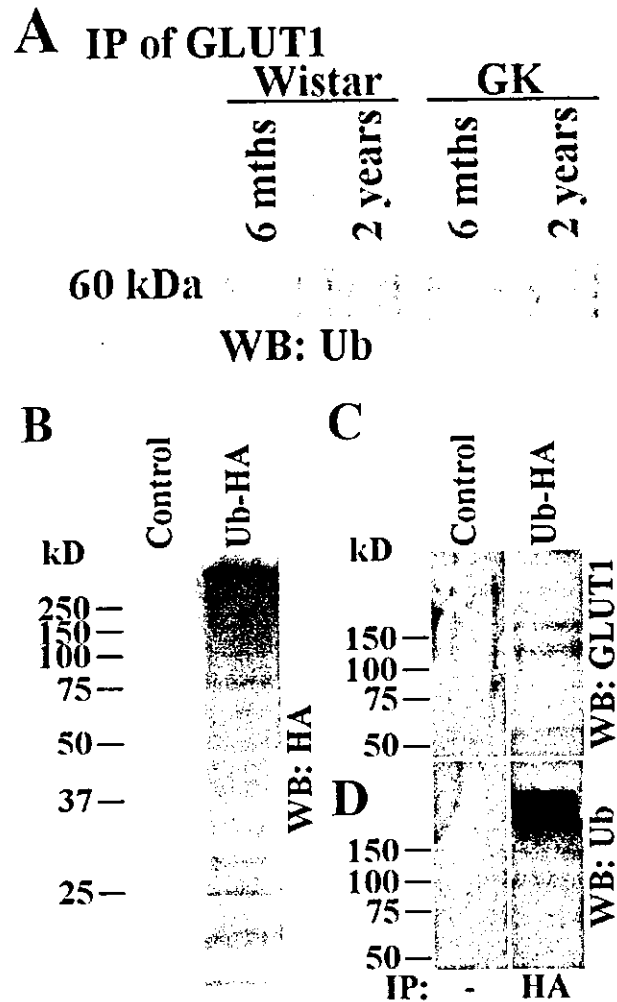


Figure 5. Evidence for ubiquitinylation of GLUT1 in vivo. A: GLUT1 was immunoprecipitated from retinal lysates obtained from Wistar (control) and GK (diabetic) rats. Proteins were resolved by SDS-PAGE, transferred to PVDF membranes, and probed with antibodies directed against ubiquitin conjugates (FK2). The additional band with molecular weight around 60 kDa is compatible with a monoubiquitinated form of GLUT1. B: HEK cells were transfected with multiubiquitin tagged to HA (Ub-HA). The cells were lysed and their proteins were resolved by SDS-PAGE, transferred to PVDF membranes, and probed with antibodies directed against HA. This showed efficient transfection and formation of endogenous Ub-HA conjugates had occurred. C: Immunoprecipitates of Ub-HA conjugates were subsequently probed with antibodies directed against GLUT1. D: Samples were immunoprecipitated with anti-HA and probed with antibodies directed against ubiquitin conjugates.

GLUT1 content as compared to control cells. This observation is consistent with the putative increase in GLUT1 degradation observed in animal models of diabetes.

Considering the practical limitations associated with the use of primary cultures of retina endothelial cells, we chose to use the TR-iBRB, which have been described as a good model for endothelial cells of inner blood-retinal barrier [7]. To investigate whether TR-iBRB would show a similar glucose-dependent decrease of GLUT1, cells were incubated either in the presence of 5.5 mM or 25 mM (hyperglycemia) glucose.

The proteins from TR-iBRB cells were separated by SDS-PAGE, transferred to PVDF membranes and probed with antibodies against GLUT1 (Figure 3A). The data are presented as percentage of the control after 1 h of incubation. After 48 h of incubation, cells treated with high glucose showed a significant decrease ($p < 0.05$) in the content of GLUT1 ($90.6 \pm 7.08\%$) as compared to control cells ($165 \pm 8.38\%$).

The expression of GLUT1 mRNA in high glucose treated TR-iBRB cells was evaluated by northern blotting. The data presented in Figure 3B show the amount of mRNA as percentage of controls after 1 h of incubation. There is no significant change in the levels of GLUT1 mRNA between the cells incubated in medium containing high and low glucose.

Diabetes is associated with increased ubiquitinylation of retinal proteins: The levels of GLUT1 of diabetic animals are lower compared to control animals (Figure 1A,B) and incubation of cultured endothelial cells in hyperglycemic conditions leads to a decrease on the GLUT1 expression (Figure 2, Figure 3A). However, in none of the tested conditions was there a significant change in the levels of mRNA for GLUT1 (Figure 1C, Figure 3B). These data led us to hypothesize that the stability of GLUT1 is decreased in diabetes or under hyperglycemia. Since the ubiquitin conjugating system is one of the proteolytic systems involved in regulating protein stability [18,19], we looked for evidence of increased ubiquitinylation in retinas of diabetic animals.

Membrane protein fractions from 6 months and 2 years old GK and WS rats were separated by SDS-PAGE, transferred to PVDF membranes and probed with antibodies directed against ubiquitin. The ubiquitinated high molecular weight conjugates were more abundant in the GK rats than in age matched WS rats (Figure 4A). When TR-iBRB cells were exposed to hyperglycemia for 15 days, a slight increase on the total amount of endogenous high molecular weight ubiquitin conjugates was observed, compared to those observed in euglycemic conditions, with a paralleled decrease in the GLUT1 content (Figure 4C), consistent with what was observed for the animal models of diabetes (Figure 4A). The endogenous ubiquitin conjugates were analysed after 15 days of high glucose treatment since only at this time point a significant increase in endogenous ubiquitin conjugates could be observed whereas GLUT1 content decreases after 48 h of incubation with high glucose (Figure 3A).

Conjugation of ubiquitin to GLUT1 is associated with increased degradation of the protein in endothelial cells: Since data show that diabetes is associated with an increase on the amount of ubiquitin-protein conjugates in the retina of rats

and in TR-iBRB cells exposed to high glucose, we further investigated whether such an increase on ubiquitin-protein conjugates is associated with an increase in the ability of retinal endothelial cell lysates to conjugate exogenous ubiquitin to endogenous substrates. Ubiquitin conjugating activity was evaluated as the ability of retinal lysates to conjugate exogenous radiolabeled ubiquitin (^{125}I -Ub) to endogenous substrates. Data presented in Figure 4B show that retinal lysates from diabetic animals present an increase of about 45% in the ability to conjugate exogenous ubiquitin to endogenous substrates. This increase in conjugation activity is reflected by the accumulation of high molecular weight ubiquitinated proteins in retinas from diabetic animals (Figure 4B). The formation of protein-ubiquitin conjugates is ATP-dependent, since there are not any conjugates formed in the absence of ATP (Figure 4B, compare "Buffer A" with "Buffer ATP").

We further evaluated the ubiquitin conjugating activity in the TR-iBRB cells exposed to high glucose. Consistent to what was observed for retinas of diabetic animals, the cytosolic fractions from TR-iBRB cells treated with high glucose concentrations showed a higher ability (approximately 28%) to form de novo ubiquitin conjugates as compared to cells treated in euglycemic concentrations (Figure 4D).

Since the proteasome is inhibited during the conjugation assays, the above data further suggest that the increase in endogenous ubiquitin conjugates in hyperglycemic conditions (GK rats and TR-iBRB cells treated with high glucose) is most likely associated with an increase on the amount of substrates prone to ubiquitinylation or an up-regulation of the activity and/or conjugating enzymes.

To investigate a possible association between GLUT1 and ubiquitin, the retinal membrane extracts from GK and WS rats were used to immunoprecipitate (IP) GLUT1. Immunoprecipitated proteins were separated by SDS-PAGE, transferred to PVDF and probed with antibodies directed against ubiquitin. A band of molecular weight near 60 kDa was detected. Because ubiquitin has a molecular mass of 8.6 kDa, this 60 kDa protein is likely to correspond to a monoubiquitinated form of GLUT1 since its molecular weight is consistent with the addition of one ubiquitin molecule to GLUT1. Interestingly, this band is more intense in the 2 year old animals (GK and WS rats) than in the 6 month old rats (Figure 5A). This probably indicates that GLUT1 is ubiquitinated in an age-dependent way and that diabetes creates the conditions that further lead to an enhanced conjugation of ubiquitin to GLUT1. To further investigate the hypothesis that GLUT1 is ubiquitinated in vivo, we transfected HEK293 cells with a HA-tagged ubiquitin cDNA, and the cell lysates were analysed to confirm efficient ubiquitinylation of cell proteins with HA-tagged ubiquitin (Figure 5B). The extracts were also used to immunoprecipitate protein-ubiquitin conjugates with an antibody against the HA epitope. Proteins were resolved by SDS-PAGE, transferred to PVDF, and the membrane was probed with antibodies against GLUT1 (Figure 5C) or against ubiquitin (Figure 5D). The immunoblot analysis showed that GLUT1 is co-precipitated with ubiquitin-HA (Figure 5C). The high molecular weight bands that cross reacted with the anti-

GLUT1 antibody are likely to correspond to ubiquitinated GLUT1. A band of approximately 50 kDa, attributed to unmodified GLUT1, is also present in the HA-ubiquitin immunoprecipitates. The presence of this band in HA immunoprecipitates may indicate that GLUT1 interacts *in vivo* with a protein that is involved in the ubiquitin proteasome pathway and that is most likely ubiquitinated *in vivo*.

DISCUSSION

The regulation of GLUT1 levels in retinal endothelial cells subjected to chronic hyperglycemia remains a matter of controversy, since there are conflicting reports in the literature [4,6,20].

In this study, we used two different animal models of diabetes, as well as a primary culture of endothelial cells and a cell line that expresses GLUT1. To mimic hyperglycemia endothelial cells were exposed to high glucose, in order to clarify the effect of diabetes on the level of expression of GLUT1. We showed that the amount of GLUT1 present in membrane fractions isolated from whole retinas of diabetic rats or rabbits is subnormal. Our data are in agreement with the results reported by Tang et al [21], showing a decrease in GLUT1 expression in retinal vascular endothelium (55%) and in homogenates of whole retina (36%) of streptozotocin-induced diabetic rats. Consistently, the results of Badr et al. showed that streptozotocin-induced diabetes reduced GLUT1 expression in the retina and its microvasculature by approximately 50% [4]. However, ultrastructural localization of GLUT1 showed increased expression of GLUT1 transporter in retinal capillaries of three diabetic patients [20]. Apparently, such contradictory observations could be due to the different approaches used to quantify GLUT1. In fact, as shown by the present data, other studies in whole retinal vasculature homogenates suggest a decrease in GLUT1 expression caused by diabetes in several different diabetic models [4,21]. On the other hand, ultrastructural localization of GLUT1 and quantification of GLUT1 sites at the capillary membranes detected either increased GLUT1 levels [20] or no changes in GLUT1 levels [22] in diabetes. Taken together, these observations suggest that the decrease on total pool of GLUT1 caused by diabetes (reported by Badr et al [4] and the present data) may not limit GLUT1 targeting to plasma membranes but may result in a reduction on the available pool of intracellular GLUT1 that could eventually compromise efficient recycling of the transporter.

The observation that hyperglycemic conditions induce a significant decrease on the amount of GLUT1 protein without significant changes on the levels of its mRNA led us to hypothesize that such decreased levels of GLUT1 may result from an increase on the degradation rate of the protein. Alterations in protein turnover during diabetes have been previously correlated with increased activity of the ubiquitin-dependent proteolytic system in skeletal [23,24] and cardiac [25] muscle. Moreover, the severity of electroneurographic changes in patients with *type 2* diabetes has been correlated with increased serum ubiquitin levels [26]. Our results show that both retinal extracts from GK rats and TR-iBRB cells treated with

high glucose present increased levels of ubiquitin conjugates as compared to controls (Figure 4A,C). The increase in the endogenous ubiquitin conjugates seems to be associated with an increased ubiquitin conjugating activity as revealed by the increased ability of tissue or cell extracts to conjugate exogenous ubiquitin to endogenous substrates (Figure 4B,D). This suggests that, in agreement to what has been observed for other tissues particularly affected by diabetes, there is an accumulation of ubiquitin conjugates and an increase in the ubiquitin conjugating activity in the retina during diabetes. Importantly these alterations can be mimicked by exposing primary culture of endothelial cells or a retinal endothelial cell line to high concentrations of glucose. The use of primary cultures of retinal endothelial cells further showed that GLUT1 in endothelial cells responds to high glucose in a manner similar to that observed for entire retinas of diabetic animals.

Since our data suggest increased degradation of GLUT1 during diabetes (Figure 1, Figure 2, and Figure 3) and since we observed an increase on ubiquitin conjugates in hyperglycemic conditions, we tested whether ubiquitinylation is the mechanism targeting GLUT1 degradation.

GLUT1 immunoprecipitated from membrane protein fractions of control and diabetic rats cross-reacts with antibodies to ubiquitin on western blots. This suggests that a ubiquitin-like modification occurs in GLUT1, particularly in the older (control and diabetic) animals. A more detailed evaluation of the role of ubiquitinylation on targeting GLUT1 for degradation was performed in TR-iBRB cells.

The immunoprecipitates of ubiquitin-protein conjugates from cells overexpressing hemagglutinin-tagged ubiquitin also revealed crossreactivity with antibodies directed against GLUT1. The presence in the HA-ubiquitin immunoprecipitates of several bands that crossreact with anti-GLUT1 antibody could be due to the uncomplete processing of the construct of multiubiquitins in the transfected cells. This approach showed that GLUT1 is ubiquitinated, but it does not allow us to ascertain whether it is mono or polyubiquitinated. We suggest that ubiquitin is the triggering signal that targets the glucose transporter GLUT1 for degradation either by lysosomes or proteasomes.

The ubiquitin proteasome pathway is involved in virtually all aspects of cell regulation [27]. The ubiquitin-dependent proteolytic pathway involves covalent conjugation of ubiquitin to substrates in a process dependent on ATP. Whereas it has been clearly established that, in most cases, conjugation of a protein to ubiquitin results in its degradation by the 26S proteasome, it has more recently been suggested that monoubiquitinylation is associated with lysosomal degradation of targeted proteins [28,29].

More recently, several proteins have been identified as being highly homologous to ubiquitin. Sentrin (or SUMO-1) is a small ubiquitin-like protein [30]. To date only six main substrates for sentrin have been characterized in mammalian cells. Whereas it has been clearly established that in most cases conjugation of a protein to ubiquitin results in its degradation by the proteasome, it has more recently been suggested that conjugation of sentrin to protein substrates, through Ubc9, is

associated with changes in its subcellular distribution [31]. Recently it was shown that both GLUT1 and GLUT4 are modified by scnturin in skeletal muscle cells and that the specialized conjugating enzyme, Ubc9, differentially regulates the cellular levels of the two GLUTs [32]. Overexpression of mUbc9 in these cells resulted in a decrease in GLUT1 abundance, presumably by targeting the protein for degradation.

We show that GLUT1 is ubiquitinated in the retina and in endothelial cells and that aging and, significantly, diabetes are associated with an increased ubiquitinylation of GLUT1. By analogy to several other membrane proteins we can suggest that GLUT1 is most likely monoubiquitinated and presumably degraded by lysosomes.

In conclusion, ubiquitinylation plays a role in the regulation of GLUT1 levels in endothelial cells in hyperglycemia and may ultimately constitute a novel level of regulation through which glucose transport into endothelial cells may transduce pathophysiological changes associated with diabetic retinopathy.

ACKNOWLEDGEMENTS

We thank Professor João Patrício and coworkers (Laboratory Animals Research Center, University Hospital, Coimbra, Portugal) for maintaining the animals.

RF was the recipient of a Fellowship from Foundation for Science and Technology, Portugal (PRAXIS XXI/BD/15583/98). This work was also supported by grants from Luso-American Foundation for Development and Portuguese Foundation for Science and Technology (FCT; Programme POCTI).

REFERENCES

- King GL, Kunisaki M, Nishio Y, Inoguchi T, Shiba T, Xia P. Biochemical and molecular mechanisms in the development of diabetic vascular complications. *Diabetes* 1996; 45:S105-8.
- Lorenzi M. Glucose toxicity in the vascular complications of diabetes: the cellular perspective. *Diabetes Metab Rev* 1992; 8:85-103.
- Kumagai AK, Glasgow BJ, Partridge WM. GLUT1 glucose transporter expression in the diabetic and nondiabetic human eye. *Invest Ophthalmol Vis Sci* 1994; 35:2887-94.
- Badr GA, Tang J, Ismail-Beigi F, Kern TS. Diabetes downregulates GLUT1 expression in the retina and its microvessels but not in the cerebral cortex or its microvessels. *Diabetes* 2000; 49:1016-21.
- Mandarino LJ, Finlayson J, Hassell JR. High glucose downregulates glucose transport activity in retinal capillary pericytes but not endothelial cells. *Invest Ophthalmol Vis Sci* 1994; 35:964-72.
- Busik JV, Olson LK, Grant MB, Henry DN. Glucose-induced activation of glucose uptake in cells from the inner and outer blood-retinal barrier. *Invest Ophthalmol Vis Sci* 2002; 43:2356-63.
- Hosoya K, Tomi M, Ohtsuki S, Takanaga H, Ueda M, Yanai N, Obinata M, Terasaki T. Conditionally immortalized retinal capillary endothelial cell lines (TR-iBRB) expressing differentiated endothelial cell functions derived from a transgenic rat. *Exp Eye Res* 2001; 72:163-72.
- Hershko A, Ciechanover A, Heller H, Haas AL, Rose IA. Proposed role of ATP in protein breakdown: conjugation of protein with multiple chains of the polypeptide of ATP-dependent proteolysis. *Proc Natl Acad Sci U S A* 1980; 77:1783-6.
- Kumagai AK, Kang YS, Boado RJ, Partridge WM. Upregulation of blood-brain barrier GLUT1 glucose transporter protein and mRNA in experimental chronic hypoglycemia. *Diabetes* 1995; 44:1399-404.
- Boado RJ, Partridge WM. The brain-type glucose transporter mRNA is specifically expressed at the blood-brain barrier. *Biochem Biophys Res Commun* 1990; 166:174-9.
- Goto Y, Suzuki K, Ono T, Sasaki M, Toyota T. Development of diabetes in the non-obese NIDDM rat (GK rat). *Adv Exp Med Biol* 1988; 246:29-31.
- Agarh CD, Agarh E, Zhang H, Ostenson CG. Altered endothelial/pericyte ratio in Goto-Kakizaki rat retina. *J Diabetes Complications* 1997; 11:158-62.
- Miyamoto K, Ogura Y, Nishiwaki H, Matsuda N, Honda Y, Kato S, Ishida H, Seino Y. Evaluation of retinal microcirculatory alterations in the Goto-Kakizaki rat. A spontaneous model of non-insulin-dependent diabetes. *Invest Ophthalmol Vis Sci* 1996; 37:898-905.
- Sone H, Kawakami Y, Okuda Y, Sekine Y, Honmura S, Matsuo K, Segawa T, Suzuki H, Yamashita K. Ocular vascular endothelial growth factor levels in diabetic rats are elevated before observable retinal proliferative changes. *Diabetologia* 1997; 40:726-30.
- Goto Y, Kakizaki M, Masaki N. Spontaneous diabetes produced by selective breeding of normal wistar rats. *Proc Jpn Acad* 1975; 51:80-5.
- Engerman RL, Bloodworth JM Jr. Experimental diabetic retinopathy in dogs. *Arch Ophthalmol* 1965; 73:205-10.
- Vinorez SA, Derevanik NL, Mahlow J, Berkowitz BA, Wilson CA. Electron microscopic evidence for the mechanism of blood-retinal barrier breakdown in diabetic rabbits: comparison with magnetic resonance imaging. *Pathol Res Pract* 1998; 194:497-505.
- Horak J. The role of ubiquitin in down-regulation and intracellular sorting of membrane proteins: insights from yeast. *Biochim Biophys Acta* 2003; 1614:139-55.
- Desterro JM, Rodriguez MS, Hay RT. Regulation of transcription factors by protein degradation. *Cell Mol Life Sci* 2000; 57:1207-19.
- Kumagai AK, Vinorez SA, Partridge WM. Pathological upregulation of inner blood-retinal barrier GLUT1 glucose transporter expression in diabetes mellitus. *Brain Res* 1996; 706:313-7.
- Tang J, Zhu XW, Lust WD, Kern TS. Retina accumulates more glucose than does the embryologically similar cerebral cortex in diabetic rats. *Diabetologia* 2000; 43:1417-23.
- Fernandes R, Suzuki K, Kumagai AK. Inner blood-retinal barrier GLUT1 in long-term diabetic rats: an immunogold electron microscopic study. *Invest Ophthalmol Vis Sci* 2003; 44:3150-4.
- Rodriguez T, Busquets S, Alvarez B, Carb N, Agell N, Lopez-Soriano FJ, Argils JM. Protein turnover in skeletal muscle of the diabetic rat: activation of ubiquitin-dependent proteolysis. *Int J Mol Med* 1998; 1:971-7.
- Galban VD, Evangelista EA, Migliorini RH, do Carmo Kettelhut I. Role of ubiquitin-proteasome-dependent proteolytic process in degradation of muscle protein from diabetic rabbits. *Mol Cell Biochem* 2001; 225:35-41.
- Liu Z, Miers WR, Wei L, Barrett FJ. The ubiquitin-proteasome proteolytic pathway in heart vs skeletal muscle: effects of acute diabetes. *Biochem Biophys Res Commun* 2000; 276:1255-60.
- Akarsu E, Pirim I, Capoglu I, Deniz O, Akcay G, Unuvar N. Relationship between electroneurographic changes and serum ubiquitin levels in patients with type 2 diabetes. *Diabetes Care*

- 2001; 24:100-3.
27. Kornitzer D, Ciechanover A. Modes of regulation of ubiquitin-mediated protein degradation. *J Cell Physiol* 2000; 182:1-11.
 28. Hlicke L. A new ticket for entry into budding vesicles-ubiquitin. *Cell* 2001; 106:527-30.
 29. Hlicke L, Dunn R. Regulation of membrane protein transport by ubiquitin and ubiquitin-binding proteins. *Annu Rev Cell Dev Biol* 2003; 19:141-72.
 30. Matunis MJ, Coutavas E, Blobel G. A novel ubiquitin-like modification modulates the partitioning of the Ran-GTPase-activating protein RanGAP1 between the cytosol and the nuclear pore complex. *J Cell Biol* 1996; 135:1457-70.
 31. Matunis MJ, Wu J, Blobel G. SUMO-1 modification and its role in targeting the Ran GTPase-activating protein, RanGAP1, to the nuclear pore complex. *J Cell Biol* 1998; 140:499-509.
 32. Giorgino F, de Robertis O, Laviola L, Montrone C, Perrini S, McCowen KC, Smith RJ. The sentrin-conjugating enzyme mUbc9 interacts with GLUT4 and GLUT1 glucose transporters and regulates transporter levels in skeletal muscle cells. *Proc Natl Acad Sci U S A* 2000; 97:1125-30.

The print version of this article was created on 30 Aug 2004. This reflects all typographical corrections and errata to the article through that date. Details of any changes may be found in the online version of the article.

RAPID
COMMUNICATION

Application of magnetically isolated rat retinal vascular endothelial cells for the determination of transporter gene expression levels at the inner blood–retinal barrier

Masatoshi Tomi and Ken-ichi Hosoya

Faculty of Pharmaceutical Sciences, Toyama Medical and Pharmaceutical University, Sugitani, Toyama, Japan

Abstract

The purpose of the present study was to quantify transporter gene levels at the inner blood–retinal barrier (inner BRB) using a combination of magnetic isolation method for rat retinal vascular endothelial cells (RVEC) and real-time quantitative PCR analysis. The transcript levels of CD31, Tie-2, claudin-5, occludin, Jam-1, mdr1a, oatp2, and oatp14 in the RVEC fraction were more than 100-fold greater than those in the non-RVEC fraction, suggesting that these genes are predominantly expressed at the inner BRB. The transcript levels of GLUT1 and MCT1 in the RVEC fraction

were the most abundant in the respective transporter family, suggesting that GLUT1 and MCT1 play a predominant role in D-glucose and monocarboxylate transport, respectively, at the inner BRB. In conclusion, application of magnetically isolated RVEC is able to determine transporter gene levels at the inner BRB thereby increasing our understanding of inner BRB functions at a molecular level.

Keywords: CD31, inner blood–retinal barrier, retinal vascular endothelial cells, magnetic beads coated antibody, transporter. *J. Neurochem.* (2004) 91, 1244–1248.

The inner blood–retinal barrier (inner BRB) forms complex tight junctions of retinal vascular endothelial cells (RVEC) to restrict non-specific transport between the circulating blood and neural retina. Therefore, transporters at the inner BRB play essential roles in supplying nutrients to the retina and are responsible for the efflux of neurotransmitter metabolites from the retina to maintain neural functions. It is important to elucidate the transporter expression and expression levels at the inner BRB in order to understand their physiological roles and design improved systems for drug delivery to the retina. Primary cultured and immortalized RVEC have been used to study transporter expression and transport functions as an *in vitro* model of the inner BRB (Greenwood 1992; Hosoya *et al.* 2004; Nakashima *et al.* 2004). Although it is easy to carry out transport studies and measure the mRNA expression of transporters by RT-PCR analysis, there is no way of knowing whether transporter expression levels are changed by culture passages and conditions. Immunohistochemical analysis and *in situ* hybridization have been used to identify transporter protein and mRNA, respectively, at the inner BRB *in vivo* (Gerhart *et al.* 1999; Gao *et al.* 2002). However, there are some limitations in studying the quantification of transporters due to the complexity of the method and its poor sensitivity.

It is thought that isolation of RVEC simplifies the investigation of the gene expression profile at the inner BRB *in vivo*. Nevertheless, this technique has not been applied to the quantification of transporters. It is difficult to obtain enough purified RVEC as RVEC represents a small percentage of the weight of the entire retina and the retina itself is a very small tissue. The cell surface antigen CD31 (platelet-endothelial cell adhesion molecule-1; PECAM-1) is exclusively and extensively expressed on the membrane of endothelial cells (Scholz and Schaper 1997). Therefore, magnetic beads coated with anti-CD31 antibodies are able to collect highly purified endothelial cells from a tissue homogenate using a magnet (Demeule *et al.* 2001). Su *et al.* (2003) applied this technique to establish primary cultured mouse RVEC and obtained an

RVEC purity of almost 100%, as determined by two endothelial markers and FACS analysis. Quantitative real-time PCR analysis means that mRNA levels can be quantified in a very sensitive manner. Therefore, a combination of magnetic isolation of highly purified RVEC and quantitative real-time PCR analysis allows the determination of transporter mRNA levels at the inner BRB *in vivo*. This is an important method which allows us to examine the molecular levels of transporters at the inner BRB, in addition to *in vitro* and *in vivo* functional transport studies.

The purpose of the present study was to isolate rat RVEC using magnetic beads coated with anti-rat CD31 antibodies, and quantify the transcript level of endothelial markers, tight junction proteins, and transporters at the inner BRB.

Materials and methods

Animals

Male Wistar rats, weighing 250–300 g, were purchased from SLC (Shizuoka, Japan). The investigations using rats described in this report conformed to the provisions of the Animal Care Committee, Toyama Medical & Pharmaceutical University (# 2003–48) and the ARVO Statement on the Use of Animals in Ophthalmic and Vision Research.

Received August 3, 2004; revised manuscript received August 25, 2004; accepted August 26, 2004.

Address correspondence and reprint requests to K. Hosoya, Faculty of Pharmaceutical Sciences, Toyama Medical and Pharmaceutical University, 2630, Sugitani, Toyama, 930-0194, Japan. E-mail: hosoyak@ms.toyama-mpu.ac.jp

Abbreviations used: BRB, blood–retinal barrier; CRT, creatine transporter; GLUT, glucose transporter; MCT, monocarboxylate transporter; mdr, multidrug resistance protein; oatp, organic anion transporting polypeptide; RVEC, retinal vascular endothelial cells; SM, smooth muscle.

Isolation of RVEC

RVEC isolation was performed using a modification of the procedure described by Su *et al.* (2003) with affinity purification using magnetic beads coated with anti-rat CD31 antibodies. Mouse anti-rat CD31 antibodies (Chemicon, Temecula, CA, USA) were incubated with Dynabeads pan mouse IgG (DynaL Biotech, Lake Success, NY, USA) overnight at 4°C to prepare magnetic beads coated with anti-rat CD31 antibodies. Rat retinas were minced and digested in 0.1% collagenase type I (Invitrogen, Carlsbad, CA, USA) and 0.01% DNase I (Roche, Mannheim, Germany) in Ca²⁺- and Mg²⁺-free Hank's balanced salt solution (HBSS) for 30 min at 37°C with agitation. Digests were filtered through a 30 µm nylon mesh, and then centrifuged at 200 × g for 10 min. The pellets were resuspended in Dulbecco's modified Eagle's medium containing 10% fetal bovine serum and incubated with magnetic beads coated with anti-rat CD31 antibodies for 1 h at room temperature. RVEC labeled with the magnetic beads were positively selected by affinity binding to the magnet.

Quantitative real-time PCR analysis

Quantitative real-time PCR was performed using an ABI PRISM 7700 sequence detector system (PE-Applied Biosystems, Foster City, CA, USA) with 2X SYBR Green PCR Master Mix (PE-Applied Biosystems) as described in a previous report (Hosoya *et al.* 2004) and gene specific primers (Table 1) through 40 cycles of 94°C for 30 s, 55–60°C for 30 s, and 72°C for 1 min. A standard curve was generated for each run using variety amounts of the plasmid containing the target gene. This enabled to quantify the initial copy number of target mRNA in the samples despite the different PCR condition of target genes. Each mRNA expression level was normalized with respect to the β-actin mRNA expression.

Results and discussion

Endothelial markers

In order to isolate RVEC from the retinal homogenate, magnetic beads coated with anti-rat CD31 antibodies were used and the magnetically collected and non-collected cells were isolated as RVEC and non-RVEC fractions, respectively. Endothelial specific markers, such as CD31 (Scholz and Schaper 1997) and Tie-2, endothelial specific receptor tyrosine kinase, were first analyzed to confirm for concentration of RVEC (Table 2). The transcript level of CD31 in the RVEC fraction was 270-fold greater than that in the non-RVEC fraction. Moreover, the expression of Tie-2 mRNA was only detected in the RVEC fraction, and not in the non-RVEC fraction. Claudin-5 and occludin are exclusively localized at the inner BRB to form tight junction strands (Morcos *et al.* 2001; Barber and Antonetti 2003). Junctional adhesion molecule-1 (Jam-1) also takes part in the formation of tight junctions, together with claudin-5 and occludin. The transcript level of claudin-5, occludin and Jam-1 in the RVEC fraction was 2,830-, 106-, and 127-fold greater, respectively, than that in the non-RVEC fraction. These results suggest that RVEC in the RVEC fraction is concentrated more than 100-fold compared with the non-RVEC fraction.

Non-endothelial markers

Glial cells markers, such as S-100β and glutamine synthetase, and a neuronal marker of neurofilament heavy chain were examined in the RVEC fraction (Table 2). The transcript level of S-100β, glutamine synthetase, and neurofilament heavy chain in the RVEC fraction was 7.3–33-fold less than that in the non-RVEC fraction, suggesting that less than 10% of the RVEC fraction is the glial and neuronal cells. In the case

Table 1 Oligonucleotide primers used for PCR amplification of cDNAs

Target mRNA	Accession Number	Upstream primer (5' to 3')	Downstream primer (5' to 3')	Product size
CD31 (PECAM-1)	RNU77697	CTT CAC CAT CCA GAA GGA AGA GAC	CAC TGG TAT TCC ATG TCT CTG GTG	360 bp
Tie-2	NM_013690*	GGG CAA AAA TGA AGA CCA GCA C	GCA TCC ATC CGT AAC CCA TCC T	516 bp
Claudin-5	XM_344058	GCA GAG CAC CGG GCA CAT GC	TAG TTC TTC TTG TCG TAA TCG CC	483 bp
Occludin	NM_031329	GCC TTT TGC TTC ATC GCT TCC	AAC AAT GAT TAA AGC AAA AGC CAC	351 bp
Jam-1	NM_053796	ACA GCC ATG AGG TCA GAG GCT	ACC TAG AAG ACA TTG AAG GCA TC	348 bp
S-100β	NM_013191	ATG TCT GAG CTG GAG AAG GCC	TCA CTC ATG TTC AAA GAA CTC ATG	279 bp
Glutamine synthetase	NM_017073	TAC CCG AGT GGA ACT TTG ATG	TAA AGT TGG TGT GGC AGC CTG	600 bp
Neurofilament heavy chain	NM_012607	TTG GAC CGA CTC TCA GAG GCA G	CAA TCC GAC ACT CTT CGC CTT CC	352 bp
α-Smooth muscle actin	X06801	TAT GTG TGA AGA GGA AGA CA	CAC AAT ACC AGT TGT ACG TC	463 bp
mdr1a (Abcb1a)	NM_133401	ACA GAA ACA GAG GAT CGC	CGT CTT GAT CAT GTG GCC	437 bp
mdr1b (Abcb1b)	NM_012623	ACA GAA ACA GAG GAT CGC	AGA GGC ACC AGT GTC ACT	352 bp
mdr2 (Abcb4)	NM_012690	ACA GAA ACA GAG GAT CGC	ATG CGT GCT TTC CAG CCA	384 bp
GLUT1 (Slc2a1)	NM_138827	GAT GAT GAA CCT GTT GGC CT	AGC GGA ACA GCT CCA AGA TG	503 bp
GLUT3 (Slc2a3)	NM_017102	GAC GAG AGT ATC AGG ATG TCA CAG	AGG CCA CGT AGA CCA AGA TAG CC	397 bp
GLUT4 (Slc2a4)	NM_012751	GTT ATG TGT CCA TCG TGG CCA TAT	CAG TCA TTC TCA TCT GGC CCT AAG	388 bp
MCT1 (Slc16a1)	NM_012716	GAA AAA CTC AAG TCC AAA GAG TCT	TTT CAT TGT CTT CTT GGG CTT CT	801 bp
MCT2 (Slc16a7)	NM_017302	CCT CTG CCC CCT AGC CCA TT	TCT GAG GGA GGA TTG TGT GTA TT	447 bp
Oatp1 (Slc21a1)	NM_017111	AAG GCC ATG AAC AGA ATG CAC ACT	AGA AAC AGG AAA TGA CAC AGG AGT GA	548 bp
Oatp2 (Slc21a5)	NM_131906	TAC TGC CCT ATG CAA GGC CAT GAA	AAC TAA CGC AAT CTG GCT TAA CCA A	397 bp
Oatp3 (Slc21a7)	NM_030838	CGC TTG GGA TTG GAT TAC ATG CAT	ATG AGA CAG TGG CCT TTG GAG AAT	612 bp
Oatp14 (Slc21a14)	NM_053441	CCT GGT GGC TTG GTT ACC TAA TAG	CTG CCC ATA CTG CTG CTC AAT GT	344 bp
CRT (Slc6a8)	NM_017348	GAA ATG GTG CTG GTC CTT CTT CAC	GTC ACA TGA CAC TCT CCA CCA CGA	353 bp
β-Actin	NM_031144	TCA TGA AGT GTG ACG TTG ACA TCC GT	CCT AGA AGC ATT TGC GGT GCA CGA TG	285 bp

*Represents the mouse sequence (the rat sequence has not been reported).

Target mRNA	Target mRNA/ β -actin mRNA ($\times 10^{-4}$)		Enrichment in the RVEC fraction
	RVEC fraction	Non-RVEC fraction	
Endothelial markers			
CD31 (PECAM-1)	38.7 \pm 6.5	0.143 \pm 0.018	270
Tie-2	15.4 \pm 2.0	N.D.	> 221
Claudin-5	1570 \pm 140	0.555 \pm 0.148	2830
Occludin	15.0 \pm 2.8	0.142 \pm 0.024	106
Jam-1	56.2 \pm 10.5	0.442 \pm 0.070	127
Non-endothelial markers			
S-100 β	4.02 \pm 0.46	133 \pm 16.2	0.0302
Glutamine synthetase	49.9 \pm 9.8	645 \pm 83	0.0774
Neurofilament heavy chain	0.294 \pm 0.036	2.15 \pm 0.29	0.137
α -Smooth muscle actin	5.06 \pm 1.55	0.223 \pm 0.052	22.7
Transporters			
mdr1a (Abcb1a)	38.6 \pm 5.63	N.D.	> 526
mdr1b (Abcb1b)	0.198 \pm 0.032	N.D.	> 2.71
mdr2 (Abcb4)	1.72 \pm 0.22	0.222 \pm 0.023	7.73
GLUT1 (Slc2a1)	120 \pm 42	65.4 \pm 4.3	1.83
GLUT3 (Slc2a3)	N.D.	0.313 \pm 0.019	–
GLUT4 (Slc2a4)	0.747 \pm 0.149	0.267 \pm 0.063	2.80
MCT1 (Slc16a1)	133 \pm 34	425 \pm 28	0.312
MCT2 (Slc16a7)	1.16 \pm 0.15	0.877 \pm 0.165	1.32
Oatp1 (Slc21a1)	N.D.	N.D.	–
Oatp2 (Slc21a5)	36.5 \pm 15.7	N.D.	> 242
Oatp3 (Slc21a7)	N.D.	N.D.	–
Oatp14 (Slc21a14)	51.5 \pm 8.0	1.28 \pm 0.06	40.2
CRT (Slc6a8)	7.08 \pm 0.45	41.9 \pm 10.1	0.169

Table 2 Transcript level of endothelial, non-endothelial markers, and transporters in retinal vascular endothelial cell (RVEC) and non-RVEC fractions

Enrichment in the RVEC fraction is the ratio of the target mRNA between the RVEC and non-RVEC fractions (RVEC fraction/non-RVEC fraction). When the target gene is not detected in the non-RVEC fraction, enrichment in the RVEC fraction is the ratio of the target mRNA level in the RVEC fraction and the lower limit of detection of each gene. Each value represents the mean \pm SEM of at least three different samples. N.D., not detected.

of glial cells, some cells are associated with the vasculature. Thus, it is suggested that a part of the vasculature-associated glial cells is captured along with the endothelial cells.

The transcript level of α -smooth muscle (SM) actin, which is exclusively expressed in perivascular cells like pericytes and SM cells, was 22-fold greater in the RVEC fraction than in the non-RVEC fraction (Table 2), demonstrating that some perivascular cells were also captured along with the endothelial cells. Nevertheless, it is also indicated that the transcript level of α -SM actin in the RVEC fraction is 2000-fold less than that of β -actin (5.06 versus 10^4). Retinal perivascular cells express α -SM actin more abundantly than β -actin (Bandopadhyay *et al.* 2001), and the transcript level of α -SM actin in cultured brain pericytes is 1.3-fold greater than that of β - and γ -actin (Boado and Pardridge 1994). The current results and previous report support the idea that the content of perivascular cells in the RVEC fraction is also very low. From these observations, although the RVEC fraction isolated using magnetic beads coated with anti-rat CD31 antibodies represents RVEC as far as the mRNA expression levels of endothelial markers are concerned, the RVEC fraction is contaminated with a small amount of non-RVEC cells like perivascular, glial, and neuronal cells. We have not analyzed markers of retinal pigment epithelial (RPE) cells as the retinas were separated from the RPE cell layer.

Transporters

Although multidrug resistance protein (mdr; P-glycoprotein) expression at the inner BRB has been recognized since 1992 (Greenwood 1992; Holash and Stewart 1993), the corresponding gene has not yet been identified. The transcript levels of three mdr isoforms, mdr1a (Abcb1a), mdr1b (Abcb1b),

and mdr2 (Abcb4), were examined in the RVEC and non-RVEC fractions (Table 2). As the data were represented as the copy number of target mRNA in the samples relative to that of β -actin, it is possible to compare the mRNA expression levels among genes. The expression of mdr1a was 200- and 24-fold greater than that of mdr1b and mdr2, respectively, in the RVEC fraction. No expression of mdr1a and 1b mRNA was detected in the non-RVEC fraction. Thus, this is the first evidence that mdr1a is predominantly expressed at the inner BRB as well as the blood-brain barrier (Schinkel *et al.* 1994). Quinidine and cyclosporine A, which are substrate of P-glycoprotein, undergo limited distribution to retinal tissue from the circulating blood (BenEzra and Maftzir 1990; Duvvuri *et al.* 2003). In light of these findings, mdr1a-encoding P-glycoprotein may prevent accumulation of substrate drugs in the retina.

Organic anion transporter(s) at the inner BRB may play a major role in transporting neurotransmitters and their metabolites in the retina. The transcript levels of organic anion transporting polypeptides (oatp), such as oatp1 (Slc21a1), oatp2 (Slc21a5), oatp3 (Slc21a7), and oatp14 (Slc21a14), were examined in the RVEC and non-RVEC fractions (Table 2). Oatp2 and 14 were detected in the RVEC fraction, whereas oatp1 and 3 were not. Oatp2 and 14 were predominantly expressed at the inner BRB. In the case of oatp2, our result is consistent with a previous immunohistochemical study (Gao *et al.* 2002). On the other hand, oatp14 has been identified as a blood-brain barrier specific anion transporter (Li *et al.* 2001). The present study revealed, for the first time, that oatp14 is also expressed at the inner BRB and may play an important role in transporting the neurosteroid conjugate of estradiol-D-17 β glucuronide and thyroid hormones to the neural retina as well as oatp2 (Sugiyama *et al.* 2003). Oatp3 was not detected in either the

RVEC or non-RVEC fractions. The lack of agreement between our result and the previous report needs an explanation. Although *oatp3* was cloned from the retina, poly(A)⁺ RNA is necessary to detect the expression of *oatp3* in the retina by northern blot and RT-PCR analyses because of the low level of expression (Ito *et al.* 2002).

Facilitative glucose transporter at the inner BRB mediates the transport of D-glucose and dehydroascorbic acid, which is an oxidized form of vitamin C, from the circulating blood to the retina (Takata *et al.* 1992; Hosoya *et al.* 2004). Among the GLUT family transporters, GLUT1 (Slc2a1), GLUT3 (Slc2a3), and GLUT4 (Slc2a4) are capable of transporting D-glucose and dehydroascorbic acid as substrates. Although it has been believed for a long time that GLUT1 has a major role in transporting D-glucose at the inner BRB (Takata *et al.* 1992), there are some arguments in favor of GLUT3 being expressed at the inner BRB and playing a role there (Knott *et al.* 1996; Hosoya *et al.* 2004). GLUT1 expression was the largest of three GLUTs, whereas GLUT3 was not detected in the RVEC fraction. The expression of GLUT4 was 100-fold less than that of GLUT1 (Table 2). Therefore, GLUT1 is responsible for the transport of D-glucose and dehydroascorbic acid at the rat inner BRB. The expression of GLUT1 in the non-RVEC fraction is half that in the RVEC fraction. Nevertheless, this evidence is in good agreement with the localization of GLUT1 in retinal glial and neuronal cells as well as the inner BRB (Kumagai *et al.* 1994).

The expression of monocarboxylate transporter-1 (MCT1/Slc16a1) in the RVEC fraction was 100-fold greater than that of MCT2 (Slc16a7). However, the transcript level of MCT1 in the RVEC fraction was 3-fold less than that in the non-RVEC fraction (Table 2), supporting the hypothesis that MCT1 is not concentrated at the inner BRB. In addition to this evidence of the mRNA level, Gerhart *et al.* (1999) used immunoelectron microscopy to provide morphological evidence that MCT1 was widely distributed in the retina including the inner BRB and MCT2 was largely expressed in glial cells of the retina. Moreover, we have reported that L-lactate transport was mediated by MCT1 in a conditionally immortalized rat retinal capillary endothelial cell line (Hosoya *et al.* 2001). From these observations, it appears that MCT1 plays a key role in monocarboxylate transport at the inner BRB.

We have recently reported that a creatine transporter (CRT/Slc6a8) at the inner BRB is responsible for the blood-to-retina transport of creatine (Nakashima *et al.* 2004). Although CRT mRNA was expressed in the RVEC fraction, the CRT expression level in the RVEC fraction was sixfold less than that in the non-RVEC fraction (Table 2). This result implies that CRT is also distributed to other retinal tissues in addition to the inner BRB as is MCT1. CRT may also play an important role in transporting creatine to photoreceptors as creatine appears to be concentrated in photoreceptors (Wallimann *et al.* 1986).

In conclusion, application of magnetically isolated RVEC allows the determination of transporter mRNA levels at the inner BRB *in vivo*. *Mdr1a*, *oatp2*, *oatp14*, GLUT1, and MCT1 are the respective family members predominantly expressed at the inner BRB. These transporters appear to play a physiologically significant role in transporting their substrates at the inner BRB. To the best of our knowledge, this is the first report to determine the transcript level of transporters at the inner BRB *in vivo*. These findings regarding the transporter gene levels at the inner BRB offer important information that will increase our understanding of the dominant gene for each transport system and their role in regulating the transport at the inner BRB.

Acknowledgements

This study was supported, in part, by a Grant-in-Aid for Scientific Research from the Japan Society for the Promotion of Science and a grant for Research on

Sensory and Communicative Disorders by the Ministry of Health, Labor, and Welfare, Japan. The authors thank Drs Satoko Hori and Tomoko Asashima for the plasmids containing tight junction and multidrug resistance protein genes and for valuable discussions, and Mr Akito Minamizono for technical assistance.

References

- Bandopadhyay R., Orle C., Lawrenson J. G., Reid A. R., de Silva S. and Allt G. (2001) Contractile proteins in pericytes at the blood-brain and blood-retinal barriers. *J. Neurocytol.* **30**, 35–44.
- Barber A. J. and Antonetti D. A. (2003) Mapping the blood vessels with paracellular permeability in the retinas of diabetic rats. *Invest. Ophthalmol. Vis. Sci.* **44**, 5410–5416.
- BenEzra D. and Maftzir G. (1990) Ocular penetration of cyclosporin A: the rabbit eye. *Invest. Ophthalmol. Vis. Sci.* **31**, 1362–1366.
- Boado R. J. and Pardridge W. M. (1994) Differential expression of alpha-actin mRNA and immunoreactive protein in brain microvascular pericytes and smooth muscle cells. *J. Neurosci. Res.* **39**, 430–435.
- Demcule M., Labelle M., Regina A., Berthelot F. and Beliveau R. (2001) Isolation of endothelial cells from brain, lung, and kidney: expression of the multidrug resistance P-glycoprotein isoforms. *Biochem. Biophys. Res. Commun.* **281**, 827–834.
- Duvvuri S., Gandhi M. D. and Mitra A. K. (2003) Effect of P-glycoprotein on the ocular disposition of a model substrate, quindine. *Curr. Eye Res.* **27**, 345–353.
- Gao B., Wenzel A., Grimm C., Vavricka S. R., Benke D., Meier P. J. and Reme C. E. (2002) Localization of organic anion transport protein 2 in the apical region of rat retinal pigment epithelium. *Invest. Ophthalmol. Vis. Sci.* **43**, 510–514.
- Gerhart D. Z., Leino R. L. and Drewes L. R. (1999) Distribution of monocarboxylate transporters MCT1 and MCT2 in rat retina. *Neuroscience* **92**, 367–375.
- Greenwood J. (1992) Characterization of a rat retinal endothelial cell culture and the expression of P-glycoprotein in brain and retinal endothelium *in vitro*. *J. Neuroimmunol.* **39**, 123–132.
- Holash J. A. and Stewart P. A. (1993) The relationship of astrocyte-like cells to the vessels that contribute to the blood-ocular barriers. *Brain Res.* **629**, 218–224.
- Hosoya K., Kondo T., Tomi M., Takana H., Ohtsuki S. and Terasaki T. (2001) MCT1-mediated transport of L-lactic acid at the inner blood-retinal barrier: a possible route for delivery of monocarboxylic acid drugs to the retina. *Pharmacol. Res.* **18**, 1669–1676.
- Hosoya K., Minamizono A., Katayama K., Terasaki T. and Tomi M. (2004) Vitamin C transport in oxidized form across the rat blood-retinal barrier. *Invest. Ophthalmol. Vis. Sci.* **45**, 1232–1239.
- Ito A., Yamaguchi K., Onogawa T., Unno M., Suzuki T., Nishio T., Sasano H., Abe T. and Tamai M. (2002) Distribution of organic anion-transporting polypeptide 2 (*oatp2*) and *oatp3* in the rat retina. *Invest. Ophthalmol. Vis. Sci.* **43**, 858–863.
- Knott R. M., Robertson M., Muckersie E. and Forrester J. V. (1996) Regulation of glucose transporters (GLUT-1 and GLUT-3) in human retinal endothelial cells. *Biochem. J.* **318**, 313–317.
- Kumagai A. K., Glasgow B. J. and Pardridge W. M. (1994) GLUT1 glucose transporter expression in the diabetic and nondiabetic human eye. *Invest. Ophthalmol. Vis. Sci.* **35**, 2887–2894.
- Li J. Y., Boado R. J. and Pardridge W. M. (2001) Blood-brain barrier genomics. *J. Cereb. Blood Flow Metab.* **21**, 61–68.
- Morcos Y., Hosie M. J., Bauer H. C. and Chan-Ling T. (2001) Immunolocalization of occludin and claudin-1 to tight junctions in intact CNS vessels of mammalian retina. *J. Neurocytol.* **30**, 107–123.
- Nakashima T., Tomi M., Katayama K., Tachikawa M., Watanabe M., Terasaki T. and Hosoya K. (2004) Blood-to-retina transport of creatine via creatine transporter (CRT) at the rat inner blood-retinal barrier. *J. Neurochem.* **89**, 1454–1461.
- Schinkel A. H., Smit J. J., van Tellingen O. *et al.* (1994) Disruption of the mouse *mdr1a* P-glycoprotein gene leads to a deficiency in the blood-brain barrier and to increased sensitivity to drugs. *Cell* **77**, 491–502.

- Scholz D. and Schaper J. (1997) Platelet/endothelial cell adhesion molecule-1 (PECAM-1) is localized over the entire plasma membrane of endothelial cells. *Cell Tissue Res.* **290**, 623–631.
- Su X., Sorenson C. M. and Sheibani N. (2003) Isolation and characterization of murine retinal endothelial cells. *Mol. Vis.* **9**, 171–178.
- Sugiyama D., Kusuhara H., Taniguchi H., Ishikawa S., Nozaki Y., Aburatani H. and Sugiyama Y. (2003) Functional characterization of rat brain-specific organic anion transporter (Oatp14) at the blood–brain barrier: high affinity transporter for thyroxine. *J. Biol. Chem.* **278**, 43 489–43 495.
- Takata K., Kasahara T., Kasahara M., Ezaki O. and Hirano H. (1992) Ultracytochemical localization of the erythrocyte/HepG2-type glucose transporter (GLUT1) in cells of the blood–retinal barrier in the rat. *Invest. Ophthalmol. Vis. Sci.* **33**, 377–383.
- Wallimann T., Wegmann G., Moser H., Huber R. and Eppenberger H. M. (1986) High content of creatine kinase in chicken retina: compartmentalized localization of creatine kinase isoenzymes in photoreceptor cells. *Proc. Natl Acad. Sci. USA* **83**, 3816–3819.

Review

Advances in the Cell Biology of Transport *via* the Inner Blood-Retinal Barrier: Establishment of Cell Lines and Transport Functions

Ken-ichi HOSOYA* and Masatoshi TOMI

Faculty of Pharmaceutical Sciences, Toyama Medical and Pharmaceutical University, 2630 Sugitani, Toyama 930-0194, Japan.

Received July 20, 2004

The retinal capillary endothelial cells are connected to each other by tight junctions that play a key role in permeability as the inner blood-retinal barrier (inner BRB). Thus, understanding the inner BRB transport mechanism is an important step towards drug targeting of the retina. Nevertheless, inner BRB transport studies have been very limited in number since it is not easy to use the retinal capillaries, which are very small in size, for *in vitro* transport studies. Conditionally immortalized rat retinal capillary endothelial cells (TR-iBRB), pericytes (TR-rPCT) and Müller cell lines (TR-MUL) have been established from transgenic rats harboring the temperature-sensitive simian virus 40 large T-antigen gene. These cell lines possess respective cell type markers and maintain certain *in vivo* functions. Using a combination of newly developed cell lines and *in vivo* studies, we have elucidated the mechanism whereby vitamin C, L-cystine, and creatine are supplied to the retina. TR-iBRB cells are also able to identify transporters and apply to study regulation of transporters under pathophysiological conditions. Furthermore, these cell lines permit the investigation of cell-to-cell interactions and the expression of inner BRB-specific genes between TR-iBRB and other cell lines.

Key words inner blood-retinal barrier; blood-ocular barrier; transport function; transporter; conditionally immortalized cell line; cell-to-cell interaction

The retina, which is a highly differentiated tissue playing a key role in vision, has a blood-retinal barrier (BRB) to maintain a constant milieu and shield the neural retina from the circulating blood. The BRB forms complex tight junctions of retinal capillary endothelial cells (inner BRB) and retinal pigment epithelial cells (RPE; outer BRB).^{1,2} The inner two thirds of the human retina is nourished by retinal capillaries and the remainder is covered by choriocapillaris *via* the outer BRB.³ In addition to the BRB, the blood-aqueous barrier, which is formed by epithelial barriers of the ciliary body and by the iridial endothelial cells, is present in the anterior segment of the eye to maintain aqueous humor conditions. Both barriers form the so-called blood-ocular barrier (Fig. 1).⁴

The concept of the BRB was first proposed by Schnaudigel in 1913⁵ following the classical work of Ehrlich and Goldman who discovered the blood-brain barrier (BBB).^{6,7} The inner BRB is structurally similar to the BBB and the retinal capillary endothelial cells are covered with pericytes and glial cells.² Glial Müller cells predominantly support retinal endothelial cells, although glial astrocytes play a major role in supporting endothelial functions at the BBB and also, partly, at the inner BRB (Fig. 1).⁸ Many groups have carried out detailed investigations of the transport functions at the BBB and Cornford postulated that the BBB acts as a dynamic regulatory interface.^{9–11} Since then, many influx and efflux transporters have been identified and characterized at the BBB.^{12,13} It was believed that the transport functions at the inner BRB are the same as those at the BBB. Nevertheless, information about transport functions and transporters at the inner BRB is very limited. Until 1999, only three transporters, *i.e.* facilitative D-glucose transporter (GLUT)1,¹⁴ monocarboxylate transporter (MCT)1,¹⁵ and P-glycoprotein (P-gp),¹⁶ had been identified immunohistochemically at the inner BRB. This lack of interest in this aspect of vision research is somewhat surprising, given that the inner BRB plays important roles in supplying nutrients to the

neural retina and is responsible for the efflux of neurotransmitter metabolites from the retina to maintain neural functions. *In vivo* transport studies using the Retinal Uptake Index (RUI) method have been performed to investigate solute transport into the retina.^{17–19} Although these have the advantage of being able to estimate the ability to transport solutes from the circulating blood to the retina under physiological conditions, it is difficult to distinguish between substrates that are taken up by the inner BRB and the outer BRB. In order to successfully identify the transporters and transport mechanisms at the inner BRB, we need to develop a good *in vitro* system, which accurately reflects *in vivo* transport functions. The techniques of isolation²⁰ and primary culture of bovine retinal capillaries²¹ have been applied to studies of the inner BRB. However, it is not easy to carry out a series of transport experiments since only 170–250 µg protein (capillary) can be obtained from a single bovine eye²⁰ and, recently, bovine spongiform encephalopathy has presented a serious social problem.²² Thus, it is important to develop retinal capillary endothelial cell lines which reflect *in vivo* transport functions and remain reproducible during multiple passages in order to elucidate transport mechanisms and identify transporters at the inner BRB. The results of such studies should provide useful information for the treatment of retinal vascular disease and macular pathology, as well as allowing more specific retinal drug targeting. The loss of pericytes in retinal capillaries is one of the earliest changes in diabetic retinopathy and this causes angiogenesis due to an increase in retinal endothelial cells.²³ Therefore, the growth of endothelial cells is thought to be regulated by pericytes and studies of cell-to-cell interactions between retinal endothelial cells and pericytes are important to elucidate the mechanisms responsible for the onset of diabetic retinopathy.

In this review, we shall focus on the cell characteristics, transport functions, and cell-to-cell interactions of newly developed rat retinal capillary endothelial cells, pericytes, and

* To whom correspondence should be addressed. e-mail: hosoyak@ms.toyama-mpu.ac.jp